Exotic Four-Manifolds, Corks, and Heegaard Floer Homology

A Dissertation Presented

by

Jonathan Hales

to

The Graduate School

in Partial Fulfillment of the Requirements

for the Degree of

Doctor of Philosophy

in

Mathematics

Stony Brook University

May 2013

Stony Brook University

The Graduate School

Jonathan Hales

We, the dissertation committee for the above candidate for the Doctor of Philosophy degree, hereby recommend acceptance of this dissertation.

Olga Plamenevskaya – Dissertation Advisor
Associate Professor, Department of Mathematics

Dennis Sullivan – Chairperson of Defense
Professor, Department of Mathematics

Oleg Viro
Professor, Department of Mathematics

Robert Lipshitz
Assistant Professor, University of North Carolina

This dissertation is accepted by the Graduate School.

Charles Taber
Interim Dean of the Graduate
School

Contents

Acknowledgements

I am extremely grateful to my advisors Olga Plamenevskaya and Robert Lipshitz. I am deeply grateful for their guidance, support, and patience. I feel very lucky to have to have met and studied under each of them.

The Mathematics community as a whole has been a joy to be a part of, I have befriended and learned from far too many to list here. I would like to thank Marco Golla, Jake Rasmussen, and Nathan Sanukjian in particular. Their insights and advice have had a large effect on this work. In addition, there are many friends whose impact, while harder to classify, have been substantial to my development. From graduate school - Ali Aleyasin, Anant Atyam, Benjamin Balsam, Paul Cernea, Eitan Chatav, Ying Chi, Stephen Dalton, Shane D'Mello, Patricio Gallardo, Panagiotis Gianniotis,Jan Gutt, Mark Hughes, Claudio Meneses, Raquel Aguilar, Vamsi Pingali, Chaya Rosen, Lloyd Smith, Yury Sobolev, Dror Varolin, Evan Wright, Matthew Wroten - and from college - Dmytro Karabash, Andrew Lawrie, Michael Lim, and Anna Salamon.

Finally, I would like to acknowledge the incredible support and encouragement I have received from my family. I cannot express how much they have done for me.

Abstract of the Dissertation

Exotic Four-Manifolds, Corks, and Heegaard Floer Homology

by

Jonathan Hales

Doctor of Philosophy

in

Mathematics

Stony Brook University

2013

Akbulut corks provide a topological avenue for understanding the smooth structures of a closed four-manifold. Computing the Heegaard Floer invariants is a first step towards understanding them. To this end, the Heegaard Floer homology of the bounding three-manifolds of the Mazur corks is computed.

Chapter 1

Introduction

In this thesis, we calculate the Heegaard Floer homology of the three-manifolds bounding a family of Akbulut corks with the goal of shedding light on the smooth structures of four-manifolds.

Four-manifolds exhibit a variety of unique exotic phenomena. For example, closed four-manifolds allow infinitely many diffeomorphism types for a single homeomorphism type.

> One might think of dimension 4 as representing a phase transition between low- and high-dimensional topology, where we find uniquely complicated phenomena and diverse connections with other fields.[GS99, xii]

The low-dimensional equivalence between the smooth and topological categories breaks down, while the powerful high-dimensional h-cobordism theorem has yet to take full effect. Akbulut corks come out of the failure to extend the smooth h-cobordism theorem to the fourth dimension.

In higher dimensions, the h-cobordism theorem states:

Theorem 1 *[Sma61] If W^{n+1} is an h-cobordism between the simply connected n-dimensional manifolds X_- and X_+, and $n \geq 5$, then W^{n+1} is diffeomorphic to the product $I \times X_-$. In particular, X_- is diffeomorphic to X_+.*

Among other things, the h-cobordism theorem gives us the generalized Poincaré conjecture for dimension greater than or equal to five.

The idea of the h-cobordism theorem is to find a handle body decomposition of the h-cobordism and then show the handles can all be cancelled. The difficulty with extending the h-cobordism theorem below the fifth dimension is the failure of the 'Whitney trick.' The Whitney trick is used to construct the handle body decomposition by resolving intersections between handle bodies by means of the embedded disks guaranteed by Whitney's embedding theorem for dimensions greater than 5.

Freedman was able to extend the h-cobordism theorem down to the fourth dimension for topological manifolds.

Theorem 2 *[Fre82, Theorem 1.3] A compact, 1-connected, smooth, 5-dimensional h-cobordism $(W; M, M')$ (which is a product over the possibly empty boundary ∂M) is topologically a product, i.e., W is homeomorphic to $M \times [0, 1]$.*

Freedman did this by using Casson handles in place of the standard two-handles used in the original h-cobordism theorem. In the fourth dimension, the Whitney trick still allows us to remove an intersection, but one cannot be sure a new intersection isn't created. The idea of a Casson handle is to iterate the process infinitely with the hope that the difficulties with creating

new intersections vanish in the limit. Indeed, Freedman showed this was true topologically:

Theorem 3 *[Fre82, Theorem 1.1] Any Casson handle is homeomorphic as a pair to the standard open 2-handle* $\left(D^2 \times (D^2)^\circ, \partial D^2 \times (D^2)^\circ\right)$.

A smooth extension of the h-cobordism theorem to the fourth dimension was shown to be impossible by Donaldson. The first step was his diagonalizablity theorem, which put severe restrictions on the intersection form of four-manifolds supporting a smooth structure.

Theorem 4 *[Don83, Theorem 1] If X is a smooth, compact, simply-connected oriented 4-manifold with the property that the associated form Q is positive definite. Then Q is equivalent, over the integers, to the standard diagonal form.*

Then, in [Don85] and [Don87], he used a new invariant of smooth structures, Donaldson polynomials, to show that the h-cobordism theorem could not extend to the fourth dimension for smooth manifolds. Namely, he showed two manifolds, which Freedman's theorem said were homeomorphic, had different Donaldson polynomials and were thus not diffeomorphic:

Theorem 5 *[Don87, Theorem 3.24] The Dolgachev surface is not diffeomorphic to the rational surface* $\mathbb{CP}^2 \# 9\overline{\mathbb{CP}}^2$.

Interestingly, the difficulties responsible for the failure of the smooth four dimensional h-cobordism theorem are, in some sense, contained in a sub-h-cobordism. In the context of four dimensional manifolds, this implies the

smooth structures on a given four-manifold can all be realized by means of a contractible co-dimension zero submanifold and an involution on it's boundary.

Theorem 6 *[Kir97] Let M^5 be a smooth five-dimensional h-cobordism between two simply connected, closed four-manifolds, M_0 and M_1. Then there exists a sub- h-cobordism $W^5 \subset M_5$ between $W_0 \subset M_0$ and $W_1 \subset M_1$ with the properties:*

1. *W_0 and hence W^5 and W_1 are compact contractible manifolds, and*
2. *$M - intW^5$ is a product h-cobordism, i.e. $(M_0 - intW_0) \times [0,1]$.*
3. *W_0 is diffeomorphic to W_1 by a diffeomorphism which, restricted to $\partial W_0 = \partial W_1$, is an involution.*

Definition 1.0.1 *The contractible co-dimension zero submanifold with an involution of it's boundary is a* cork *(W, τ) of a differentiable simply connected smooth four-manifold M if $M = M - W \cup_{Id} W$ is homeomorphic, but not diffeomorphic to $M' = M - W \cup_f W$.*

The act of cutting and regluing W with the involution τ is called a cork twist*.*

Corks have been found in many pairs of homeomorphic, but non-diffeomorphic, four-manifolds. The first example of a cork was found by Akbulut in [Akb91]. The Mazur manifold (W_1, τ_1) was shown to be a cork in $E(2) \# \overline{\mathbb{CP}}^2$. Subsequently, many more examples have been found. See for example [AY08] in which they show:

Theorem 7 *For $n \geq 1$,*

$$(W_{2n-1}, \tau_{2n-1}) \text{ and } (W_{2n}, \tau_{2n}) \text{ are corks in } W_{2n}.$$

The 'Mazur' corks, (W_n, τ_n) are the focus of this thesis and are the compact four-manifolds given by the Kirby diagram in figure 1.1. τ_n is given by the homeomorphism induced by swapping $0 \leftrightarrow \cdot$ on each component. Since the link is symmetric, τ_n is an involution.

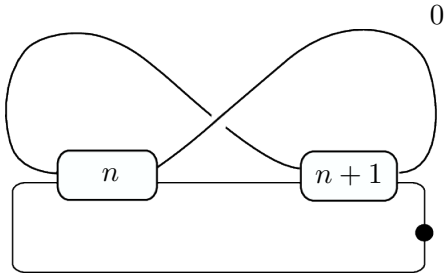

Figure 1.1: Akbulut cork W_n

The presence of a cork in a manifold does not, by itself guarantee the cork twist will produce an exotic copy. Smooth invariants are needed to distinguish smooth structures on four-manifolds with the same topological type. The Donaldson polynomials, mentioned above in theorem 5, were the first such invariant. The Donaldson polynomial's gauge theoretic approach to smooth four-manifolds was continued with the Seiberg-Witten invariant. Seiberg-Witten invariants were much easier to compute and largely superseded the use of Donaldson polynomials. In many cases, it is possible to detect different smooth structures by using properties of the invariant with respect to some extra structure. For example, a symplectic structure on a four-manifold implies the Seiberg-Witten invariant is non-vanishing.

The Heegaard Floer invariant was inspired by the power of the Seiberg-Witten invariant (in fact they are conjectured to be equivalent cf. [KLT10]) and the hope to create an invariant whose computation did not rely so heavily on the fortuitous presence of some extra structure.

The Heegaard Floer invariant is a diffeomorphism invariant for closed differentiable four-manifolds with $b_2^+ > 1$. It is built off of the Heegaard Floer homology of three-manifolds.

To a closed, oriented three-manifold, we can associate a tuple of groups : HF^-, HF^∞ and HF^+ (we give a more detailed review in chapter 2). These groups are associated with a long exact sequence:

$$... \longrightarrow HF^- \longrightarrow HF^\infty \longrightarrow HF^+ \longrightarrow ...$$

which is abbreviated with the notation HF°. There is a fourth group, HF_{red} which is defined to be either:

$$\frac{HF^+}{U^k \cdot HF^+} \qquad k >> 0$$

or

$$\ker\left(U^k : HF^- \longrightarrow HF^-\right) \qquad k >> 0.$$

HF_{red} is well defined as the two groups are isomorphic. The isomorphism is given by the boundary map, ∂_*, of the above long exact sequence [OS04d, Lemma 4.6].

HF_{red} thus gives us a way to compose maps on HF^- and HF^+, which is needed in the definition of the four-manifold invariant.

Let W be cobordism between the closed oriented three-manifolds M_0 and M_1, and $\mathfrak{t}$ a spin^c structure on W that restricts to $\mathfrak{s}_0$, $\mathfrak{s}_1$ on M_0 and M_1. In [OS06], they construct a map,

$$F^{\circ}_{W,\mathfrak{t}} : HF^{\circ}(M_0, \mathfrak{s}_0) \longrightarrow HF^{\circ}(M_1, \mathfrak{s}_1)$$

and show it is natural with respect to HF° and a smooth invariant of W and $\mathfrak{t}$. (A gap in the original proof of naturality was fixed in [JT12].)

The Heegaard Floer invariant of a closed four-manifold X with $b_2^+ > 1$ is defined as follows: Remove two four-balls from X to get a cobordism $\widehat{X}$ from $S^3 \longrightarrow S^3$. Cut $\widehat{X}$ along an embedded three-manifold N,

$$\widehat{X} = W_1 \cup_N W_2,$$

such that both $b_2^+(W_1)$ and $b_2^+(W_2) > 0$ (recall $b_s^+(X) > 1$). This condition on the Betti numbers are needed to keep the invariant independent of the cut N. The cobordism map:

$$F^-_{W_1} : HF^-\left(S^3\right) \longrightarrow HF^-(N)$$

factors through the inclusion $HF^-_{\mathrm{red}}(N) \hookrightarrow HF^-(N)$ and

$$F^+_{W_2} : HF^+\left(S^3\right) \longrightarrow HF^+(N)$$

factors through the projection $HF^+(N) \longrightarrow HF^+_{\mathrm{red}}(N)$. The isomorphism induced by ∂_* lets us compose these two maps.

The closed four-manifold invariant is the coefficient of the image of the composition of these maps evaluated on the highest graded element $\mathbf{x} \in HF^-(S^3) = \mathcal{T}^-_{(-2)}$:

$$\Phi(X, \mathfrak{t}) = F^+_{W_2} \circ \left(\partial_* |_{HF^+_{\mathrm{red}}}\right)^{-1} \circ F^-_{W_1}(\mathbf{x}).$$

(Here ∂_* is the isomorphism of the HF_{red} coming from the long exact sequence).

While the Seiberg-Witten invariants have been used with some success in studying corks, the hope is the Heegaard Floer invariants will facilitate subtler computations which do not rely on, for example, an associated symplectic structure. One hope would be to understand corks well enough to construct exotic pairs with their help. Toward this goal we compute the Heegaard Floer homology of the boundaries of the Mazur corks (figure 1.1).

There has already been work done towards this goal. In [AD05] it was shown that the map, f_* on HF^+ induced by the boundary involution acted non-trivially on the Heegaard Floer homology of first example of the Mazur corks, $HF^+(-\partial W_1)$. More recently, in [AK11], f_* was shown to act non-trivially on the contact invariant lying within the Floer homology.

Last year an algorithm to compute the Heegaard Floer homologies of the Mazur corks were given in [AK12]. They realized that, if gradings are disregarded, the homologies were found to be isomorphic to a class of plumbed three-manifolds which could be computed algorithmically using *Nemethi's method*. This thesis gives a closed form solution for this class using a different approach. This approach allows the calculation of absolute gradings, is applicable to all corks presented as two bridge links, and seems to have a

natural path to the computation of the four-manifold invariant.

Also of related interest, the Instanton Floer homology of this family of corks was recently computed as well in [Har13].

Remark 1.0.2 *For technical reasons (the preference of HF^+ over HF^-) negatively oriented corks, $-W_n$, are studied.*

The Kirby diagram of the three-manifold bounding $-W_n$ is given by replacing the 1-handle by a zero framed two handle:

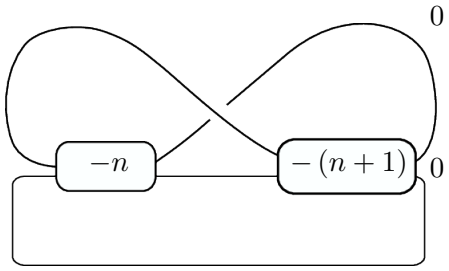

Figure 1.2: Oppositely oriented Akbulut cork boundary $-\partial W_n$

In section 3.1 the calculation is reduced from, $-\partial W_n$ (a three-manifold given by surgery on a link) to $Y^n = (S^3_{(+1)}(K^n))_1$ (a three-manifold given by surgery on a knot). A Heegaard diagram for this knot is found in chapter 3, section 3.2 and the chain complex in section 3.3. Finally, in chapter 4 we use the integer surgery formula from [OS08] to compute the Floer homology of their $+1$ surgeries, $HF^+(Y^n)$ and thus $HF^+(-\partial W_n)$.

In chapter 5 we discuss further directions for this approach and sketch the first calculation for another class popular class of corks.

The main result is:

Theorem 1.0.3

$$HF^+(-\partial W_n) = \mathcal{T}_0^+ \oplus \bigoplus_{-n<s<n} \left(\frac{\mathbb{F}[U]}{U^{m(s,0)}\mathbb{F}[U]} \right)^2_{((s^2-s)-(i^2-i)-min(0,2(i-s)))} \oplus \left(\bigoplus_{\{m(s,i)>0, i\neq 0\}} \frac{\mathbb{F}[U]}{U^{m(s,i)}\mathbb{F}[U]} \right)_{((s^2-s)-(i^2-i)-min(0,2(i-s)))}$$

Where sum is taken over U-modules distinguished by the exponent, $m(s,i)$, of the quotient:

$$m(s,i) = \begin{cases} min(0,(i-s)) - \frac{n-|i|-(s-i)+1}{2} & \text{if } n-|i|-(s-i) \text{ is odd} \\ min(0,(i-s)) - \frac{n-|i|-(s-i)}{2} & \text{if } n-|i|-(s-i) \text{ is even} \end{cases} \tag{1.1}$$

where, $|i|, |s| < n$.

Chapter 2

Background on Heegaard Floer homology

2.0.1 Heegaard Floer homology

Remark 2.0.4 *Let $\mathbb{F}$ denote $\mathbb{Z}/2\mathbb{Z}$. We will use the Floer invariant with coefficients in $\mathbb{F}$.*

Notation 2.0.5 *Recall the following commonly used U-modules:*

$\mathcal{T}^{\infty}$ will denote the $\mathbb{F}[U]$ module $\mathbb{F}[U, U^{-1}]$

$\mathcal{T}^{-}_{(d)}$ will denote the $\mathbb{F}[U]$ module $\mathbb{F}[U]$ with maximum grading d.

$\mathcal{T}^{+}_{(d)}$ will denote the $\mathbb{F}[U]$ module $\frac{\mathbb{F}[U,U^{-1}]}{U\cdot\mathbb{F}[U]}$ with minimum grading d.

Heegaard Floer homology is an invariant of a closed oriented three-manifold. A closed orientable three-manifold can be split into two handle bodies and a gluing map ϕ:

$$U_{\alpha} \cup_{\phi} U_{\beta}.$$

This splitting can be encoded by a genus g surface Σ and two g-tuples of circles - $\boldsymbol{\alpha}$, $\boldsymbol{\beta}$. The circles in $\boldsymbol{\alpha}$ (and $\boldsymbol{\beta}$) are linearly independent in homology. Attaching two-handles to the $\boldsymbol{\alpha}$, $\boldsymbol{\beta}$ circles gives U_α, U_β respectively.

If we distinguish a point z on a Heegaard diagram we call it a *pointed* Heegaard diagram:

$$(\Sigma, \boldsymbol{\alpha}, \boldsymbol{\beta}, z)\,.$$

For technical reasons related to the Floer construction, we work with pointed Heegaard diagrams.

From the pointed Heegaard diagram we form the g-fold symmetric product $\mathrm{Sym}^g(\Sigma)$. There are some technical conditions having to do with the almost complex structure we put on it, but it is shown that for a generic almost complex structure the invariant is independent of the choice of almost complex structure.

Within $\mathrm{Sym}^g(\Sigma)$ we have two totally real tori:

$$\mathbb{T}_\alpha = \alpha_1 \times ... \times \alpha_g \subset \mathrm{Sym}^g(\Sigma)$$

$$\mathbb{T}_\beta = \beta_1 \times ... \times \beta_g \subset \mathrm{Sym}^g(\Sigma)\,.$$

The chain complexes are generated over $\mathbb{F}$ by the intersection points of $\mathbb{T}_\alpha \cap \mathbb{T}_\beta$.

For $\mathbf{x}, \mathbf{y} \in \mathbb{T}_\alpha \cap \mathbb{T}_\beta$, a *Whitney disk*, $\phi \in \pi_2(\mathbf{x}, \mathbf{y})$, is an map of the unit disk $\mathbb{D}^2 \subset \mathbb{C}^2$ into $Sym^g(\Sigma)$ such that:

1. $-i \mapsto \mathbf{x}$
2. $i \mapsto \mathbf{y}$

3. $\partial\mathbb{D}^2 \cap \{x > 0\} \mapsto \mathbb{T}_\alpha$

4. $\partial\mathbb{D}^2 \cap \{x < 0\} \mapsto \mathbb{T}_\beta$.

We study the moduli space, $\mathcal{M}(\phi)$, of psuedo-holomorphic embeddings ϕ with Maslov index equal to one, $\mu(\phi) = 1$.

The Maslov index is the expected dimension of the moduli space. In general the Maslov index is hard to compute, but with the help of [Lip06] it can be computed from the diagram combinatorially.

By restricting to the moduli space with Maslov index one and the help of Gromov's compactness theorem, the quotient space $\frac{\widehat{\mathcal{M}}(\phi)}{\mathbb{R}}$ is shown to be a compact zero dimensional space. Thus the count of the holomorphic disks $\#\frac{\widehat{\mathcal{M}}(\phi)}{\mathbb{R}}$ is finite.

Definition 2.0.6 *$CF^\infty(\Sigma, \boldsymbol{\alpha}, \boldsymbol{\beta}, z)$ is the module freely generated over $\mathbb{F}$ by generators $[\mathbf{x}, i] \in (\mathbb{T}_\alpha \cap \mathbb{T}_\beta) \times \mathbb{F}$, endowed with a differential*

$$\partial[\mathbf{x}, i] = \sum_{\mathbf{y} \in \mathbb{T}_\alpha \cap \mathbb{T}_\beta} \sum_{\{\phi \in \pi_2(\mathbf{x}, \mathbf{y}) \,\big|\, \mu(\phi) = 1\}} \#\widehat{\mathcal{M}}(\phi)[\mathbf{y}, i - n_z(\phi)].$$

Where $n_z(\phi)$ is the algebraic intersection of $z \times Sym^{g-1}$ with ϕ in $Sym^g(\Sigma)$.

In general, the differential is hard to compute as finding the holomorphic disks require the solution of partial differential equations. In our case, we will be able to restrict to a special diagram, namely a surface with genus one, in which these disks can be computed combinatorially.

Definition 2.0.7 *$CF^-(\Sigma, \boldsymbol{\alpha}, \boldsymbol{\beta}, z)$ is the subcomplex with $i < 0$:*

$$CF^- = CF^\infty \{i < 0\}.$$

CF^+ is the quotient:

$$CF^+ = \frac{CF^\infty}{CF^-}.$$

$\widehat{CF}(\Sigma, \boldsymbol{\alpha}, \boldsymbol{\beta}, z)$ is the subcomplex of CF^+:

$$\widehat{CF} = \frac{CF\{i \leq 0\}}{CF\{i < 0\}}.$$

These complexes are modules over the polynomial algebra $\mathbb{F}[U]$, where $U \cdot [\mathbf{x}, i] = [\mathbf{x}, i-1]$.

We have induced $\mathbb{F}[U]$-actions on their homology groups $HF^\infty(Y)$, $HF^-(Y)$, and $HF^+(Y)$.

The complexes have a relative $\mathbb{Z}$-grading:

$$gr(\mathbf{x}, \mathbf{y}) = \mu(\phi) - 2n_z(\phi).$$

where $\phi \in \pi_2(\mathbf{x}, \mathbf{y})$.

In our case of $b_1(Y) = 0$ this can be lifted to an absolute $\mathbb{Q}$-grading. [OS03]

Theorem 8 *[OS04d, Theorem 1.1] $\widehat{HF}$, HF^-, HF^+, HF^∞ thought of as modules over $\mathbb{F}[U]$ are topological invariants of Y.*

When $b_1(Y) > 0$ there is a mapping $\mathfrak{s} : \mathbb{T}_\alpha \cap \mathbb{T}_\beta \longrightarrow \text{spin}^c(Y)$. It can be shown that the differential, ∂, respects the partition, defined by $\mathfrak{s}$, of CF° by spin^c structures. Thus the chain complexes CF° and their homologies split into subcomplexes indexed by spin^c structure.

$$CF^\circ(Y) = \bigoplus_{\mathfrak{s}} CF^\circ(Y; \mathfrak{s})$$

Note: the boundaries of corks are integer homology spheres, so $b_1(Y) = 0$ and we can ignore issues with spin^c structures.

See [OS04d] and [OS04c] for details.

2.0.2 Knot Floer homology

An invariant of a knot K in S^3 is constructed by defining a filtration on the Heegaard Floer chain complexes. In general, the invariant is defined for a null-homologous knot in a closed, oriented three-manifold, but only the case of S^3 is used here.

Let K be an oriented knot in an integer homology sphere Y and let $(\Sigma, \boldsymbol{\alpha}, \boldsymbol{\beta}_0)$, where $\boldsymbol{\alpha} = \{\alpha_1, ..., \alpha_g\}, \boldsymbol{\beta}_0 = \{\beta_2, ..., \beta_g\}$, be a Heegaard diagram for the knot complement.

Then we will say $(\Sigma, \boldsymbol{\alpha}, \boldsymbol{\beta}_0 \cup \mu)$, where μ is the meridian of K, is a Heegaard diagram for (Y, K).

Marking a point p on μ, lets us define z and w. For a small enough neighborhood N of p, there are two conected components in $N - \mu$. Marka z and w in each of the connected components. This gives us a *doubly-pointed* Heegaard diagram for a knot (Y, K), $\mathcal{H}(\Sigma, \boldsymbol{\alpha}, \boldsymbol{\beta}, z, w)$. The choice of which component to place z and w in corresponds to the two possible orientations of the knot (so switching z an w corresponds to switching the orientation of the knot). See figure 2.1 for an example when $Y = S^3$ and K is the right handed trefoil.

Definition 2.0.8 *Because the coefficients are in $\mathbb{F} = \mathbb{Z}/2\mathbb{Z}$ we can abuse notation and use $\mathbf{x} \in \mathbb{T}_\alpha \cap \mathbb{T}_\beta$ to also refer to the algebraic elements.*

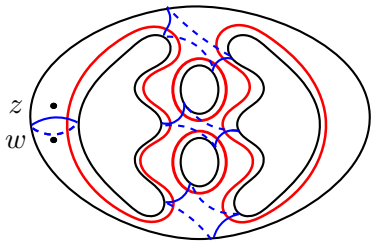

Figure 2.1: Doubly pointed Heegaard diagram for a right handed trefoil.

Let $\mathcal{R}$ *be the* $\mathbb{Z} \oplus \mathbb{Z}$ *bigraded chain complex generated over* $\mathbb{F}$ *by* $\mathbb{T}_\alpha \cap \mathbb{T}_\beta$ *with differential,*

$$\partial \mathbf{x} = \sum_{\mathbf{y} \in \mathbb{T}_\alpha \cap \mathbb{T}_\beta} \sum_{\{\phi \in \pi_2(\mathbf{x},\mathbf{y}) \,\big|\, \mu(\phi)=1\}} \#\widehat{\mathcal{M}}(\phi)\mathbf{y}. \tag{2.1}$$

$CFK^\infty(S^3, K)$ *is then the* $\mathbb{F}[U]$ *module*

$$\mathbb{F}[U, U^{-1}] \otimes \mathcal{R}.$$

We define a filtration function $\mathcal{F} : CFK^\infty \longrightarrow \mathbb{Z} \oplus \mathbb{Z}$ *by demanding*

1. *For* $\mathbf{x}, \mathbf{y} \in \mathcal{R}$, $\mathcal{F}(\mathbf{x}, \mathbf{y}) = (n_z(\phi), n_w(\phi))$, *where* $\phi \in \pi_2(\mathbf{x}, \mathbf{y})$.

2. *If we place* $\mathbf{x} \in \mathcal{R}$ *in the plane at coordinates* $\mathcal{F}(\mathbf{x})$, $\mathcal{R}$ *is symmetric across the line* $y = x$.

3. $$\mathcal{F}(\mathbf{x}, U \otimes \mathbf{x}) = (1, 1).$$

$\mathcal{F}$ *induces a* $\mathbb{Z} \times \mathbb{Z}$ *filtration on* CFK^∞ *by:* $\mathcal{F}(\mathbf{x}) \leq \mathcal{F}(\mathbf{y})$ *if and only if both the coordinates of* $\mathcal{F}(\mathbf{x})$ *are less than are equal to the coordinates of* $\mathcal{F}(\mathbf{y})$.

Projection of the filtration $\mathcal{F}$ to the x-coordinate will be denoted by: $\mathcal{F}_1(\mathbf{x},\mathbf{y})$. Projection of the filtration $\mathcal{F}$ to the y-coordinate will be denoted by: $\mathcal{F}_2(\mathbf{x},\mathbf{y})$.

This is equivalent to the filtration from [OS04a, pg. 13], the filtration will be encoded by placing the elements of the complex on a $\mathbb{Z}\times\mathbb{Z}$ lattice at coordinates given by their evaluation by $\mathcal{F}$. The differentials will represented by arrows. See figure 2.2 for an example when K is the right handed trefoil.

Remark 2.0.9 *If the Heegaard diagram for a knot has genus one, even the differentials can be computed combinatorially. This will be elaborated on in subsection 3.2.*

Remark 2.0.10 *The initial definition of CFK^∞ was given in the following equivalent form:*

Let $CFK^\infty(S^3,K)$ be the chain complex of the $\mathbb{F}[U]$ module on the free abelian group generated by the triples $[\mathbf{x},i,j]$, $\mathbf{x}\in\mathbb{T}_\alpha\cap\mathbb{T}_\beta$ and $i,j\in\mathbb{Z}$ with U-action:

$$U\cdot[\mathbf{x},i,j]=[\mathbf{x},i-1,j-1],$$

with differential,

$$\partial[\mathbf{x},i,j]=\sum_{\mathbf{y}\in\mathbb{T}_\alpha\cap\mathbb{T}_\beta}\sum_{\{\phi\in\pi_2(\mathbf{x},\mathbf{y})|\mu(\phi)=1\}}\#\widehat{\mathcal{M}}(\phi)[\mathbf{y},i-n_z(\phi),i-n_w(\phi)]. \quad (2.2)$$

$$\underline{\mathfrak{s}}(\mathbf{x})+(i-j)PD[\mu]=\underline{\mathfrak{t}}.$$

Here $\underline{\mathfrak{s}}$ corresponds to the spin^c structures of the knot complement.

Theorem 2.0.11 *[OS04a, Theorem 3.1] Let (S^3,K) be an oriented knot.*

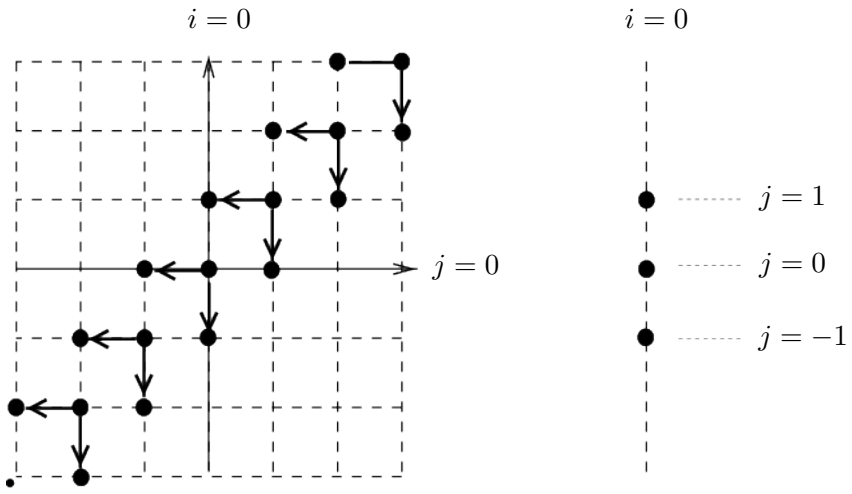

Figure 2.2: The chain complex $CFK^\infty(S^3, K)$ (left) and $\bigoplus_j \widehat{CFK}(S^3, K, j)$ (right) for right handed trefoil.

Then the filtered chain homotopy type of the chain complex $CFK^\infty(S^3, K)$ is a topological invariant of the oriented knot K.

Just as with the three-manifold invariant, the homology of the infinity variant is not particularly interesting. Knot Floer homology is generally used to refer to the hat variant, $\widehat{HFK}$. Although the homology of $CFK^\infty(Y, K)$ is generally not interesting, its chain homotopy type carries a lot of information. In particular it can be used to compute the Floer homology of knot surgeries along K (section 4).

See [OS04a] for more details on the construction of CFK^∞ and the computation of $HF^+(Y_n)$ for sufficiently large $|n|$. For the case of all $n \in \mathbb{Z}$ see [OS08].

2.0.3 Integer Surgery

Given the chain homotopy type of $CFK^\infty(S^3, K)$, [OS08] describes how to calculate the Floer homology of an integer surgery along (S^3, K). We review the details for the case of $+1$ surgery.

Theorem 2.0.12 *[OS08, Theorem 4.1] Let Y be an integral homology three-sphere. Then the homology of the mapping cone $\mathbb{X}^+(1)$ of*

$$D_1^+ \colon \mathbb{A}^+ \longrightarrow \mathbb{B}^+$$

is isomorphic to $HF^+(Y_1(K))$.

(The definition of the mapping cone follows below 2.0.14).

Remark 2.0.13 *The above theorem is abridged. The details about the grading shift and spin^c structures are skipped as the surgery coefficient of $+1$ makes the grading shift zero and the spin^c structures are trivial on an integer homology sphere.*

Definition 2.0.14 *Let:*

$$\mathcal{C}_s = \{U^m \otimes \mathbf{x} \in CFK^\infty | \mu\left(U^m \otimes \mathbf{x}\right) < 0 \text{ and } \mathcal{A}\left(U^m \otimes \mathbf{x}\right) < s\}$$

and

$$C\{i < 0\} = \{U^m \otimes \mathbf{x} \in CFK^\infty | \mu\left(U^m \otimes \mathbf{x}\right) < 0\}.$$

Define the following quotients:

$$A_s^+ = \frac{CFK^\infty}{\mathcal{C}_s}$$

$$B_s^+ = \frac{CFK^\infty}{C\{i < 0\}}$$

and maps between them:

$$v_s^+ \colon A_s^+ \longrightarrow B_s^+$$

and

$$h_s^+ \colon A_s^+ \longrightarrow B_{s+1}^+.$$

The map v_s^+ is projection onto B_s^+. h_s^+ is projection onto $C\{j \geq s\}$, which is identified with B_{s+1}^+ by multiplying by U^s, and then using the chain homotopy equivalence from $C\{j \geq 0\}$ to $C\{i \geq 0\}$. [OS08, pg. 2]

Note that B_s^+ is not dependent on the index s. The index is relevant to the

absolute grading defined below.

$\mathbb{X}^+(1)$ *is then the mapping cone of*

$$D_1^+ : \mathbb{A}^+ \longrightarrow \mathbb{B}^+$$

where

$$\mathbb{A}^+ = \bigoplus_s A_s^+$$

$$\mathbb{B}^+ = \bigoplus_s B_s^+$$

and D_1^+ *is the direct sum of the chain maps:*

$$D_1^+ = \bigoplus_s v_s^+ \oplus h_s^+.$$

The quotients of CFK^∞, A_s^+ *and* B_s^+ *inherit its absolute grading. We shift this old grading by:*

$$d \mapsto d + s(s-1) + 1. \tag{2.3}$$

The integer surgeries formula says the resulting grading on the mapping cone $\mathbb{X}^+(1)$ *gives us the absolute grading of the surgered manifold.*

Remark 2.0.15 *The* 1 *in* D_1^+, $\mathbb{X}^+(1)$, A_s^+, *and* B_s^+ *denotes we are doing* $+1$ *surgery. It is included to keep notation consistent with [OS08].*

The computation of the mapping cone is simplified greatly by *truncating* the infinite sums $\mathbb{A}^+$, $\mathbb{B}^+$ to the finite ones:

$$\mathbb{A}^+(b) = \bigoplus_{-b \le s \le b} A_s^+$$

$$\mathbb{B}^+(b) = \bigoplus_{1-b \leq s \leq b} B_s^+.$$

The truncated mapping cone is denoted:

$$\mathbb{X}^+(1; b).$$

The following lemma tells us we can always use the truncated mapping cone:

Lemma 2.0.16 *[OS08, Lemma 4.3] For b sufficiently large, $\mathbb{X}^+(1; b)$ is quasi-isomorphic to $\mathbb{X}^+(1)$. In particular, they are quasi-isomorphic if v_s^+ and h_s^+ are isomorphisms for $|s| > b$.*

2.1 Lifted Heegaard Diagram

When the genus of the Heegaard diagram is one, we can compute CFK^∞ combinatorially. This is done by looking at the lift of the Heegaard diagram, $\overline{\mathcal{H}}$.

This is very straight forward. The one subtlety is determining the combinatorial conditions for a Whitney disk to have a holomorphic representative. The condition for counting the holomorphic disks is given in the definition for the differential below. For the proof that this gives CFK^∞, see [OS04a].

Definition 2.1.1 *The cover $\overline{\mathcal{H}(K)}$ of a genus one Heegaard Diagram $\mathcal{H}(K)$:*

1. *Let D be the unit square $[0,1]\times[0,1]$ marked at two points: $\{(\frac{1}{3}, \frac{1}{2}), (\frac{2}{3}, \frac{1}{2})\}$*
2. *Let $\overline{\mathbb{R}^2}$ be a tiling of $\mathbb{R}^2$ by D. $\widetilde{\alpha}$, $\widetilde{\beta}$ be embeddings of $\mathbb{R}$.*

3.

$$\widetilde{\mathbf{z}} = \{(\mathbb{Z} + \frac{1}{3}, \mathbb{Z} + \frac{1}{2}\}$$

4.

$$\widetilde{\mathbf{w}} = \{(\mathbb{Z} + \frac{2}{3}, \mathbb{Z} + \frac{1}{2}\}$$

5. *Then denote* $\overline{\mathcal{H}} = \left(\overline{\mathbb{R}^2}, \widetilde{\alpha}, \widetilde{\beta}, \widetilde{\mathbf{w}}, \widetilde{\mathbf{z}}\right)$.

6. *If the quotient by integer translation is the Heegaard Diagram for a knot,*

$$\frac{\overline{\mathcal{H}}}{\mathbb{Z} \oplus \mathbb{Z}} \cong \mathcal{H}(K),$$

we write $\overline{\mathcal{H}(K)} = \overline{\mathcal{H}}$.

Definition 2.1.2 *The knot Floer complex* $CFK^\infty\left(\overline{\mathcal{H}(K)}\right)$ *of the cover* $\overline{\mathcal{H}(K)}$*:*

1. *The generators:*

   - *Let* $\underline{\mathfrak{s}} : \widetilde{\alpha} \cap \widetilde{\beta} \to \underline{spin^c}\,(S^3 - K)$ *be a map to the spin*^{c} *structures on the knot complement defined by* $\widetilde{\mathbf{x}} \mapsto \underline{\mathfrak{s}}(\widetilde{\mathbf{x}}) = \underline{\mathfrak{s}}\,(\pi(\widetilde{\mathbf{x}}))$. *We use this to define the generators of the complex:*
   - $CFK^\infty(\overline{\mathcal{H}(K)})$ *is generated by* $\{[\widetilde{\mathbf{x}}, i, j]|\quad \widetilde{\mathbf{x}} \in \widetilde{\alpha} \cap \widetilde{\beta}, \quad i, j \in \mathbb{Z}, \quad \underline{\mathfrak{s}}\,(\widetilde{\mathbf{x}}) + (i - j) = 0\}$

2. *The filtration:*

   - *Define a* $\mathbb{Z} \oplus \mathbb{Z}$ *filtration by*

$$\mathcal{F}[\widetilde{\mathbf{x}}, i, j] = (i, j)$$

and the ordering

$$(i,j) < (i',j') \leftrightarrow i < i' \text{ and } j < j'.$$

3. *The differential:*

   - *For* $\widetilde{\mathbf{x}}, \widetilde{\mathbf{y}} \in \widetilde{\alpha} \cap \widetilde{\beta}$ *let* $\pi_2(\widetilde{\mathbf{x}}, \widetilde{\mathbf{y}}) = \{\widetilde{\phi} : \mathbb{D} \longrightarrow \mathbb{R}^2 | \widetilde{\phi}$ *is an embedding,* $\widetilde{\phi}|_{\partial \mathbb{D}} \subset \widetilde{\alpha} \cup \widetilde{\beta}$, $\widetilde{\phi}(-i) = \widetilde{\mathbf{x}}, \widetilde{\phi}(i) = \widetilde{\mathbf{y}}\}$

   - *For* $\widetilde{\mathbf{x}} \in \widetilde{\alpha} \cap \widetilde{\beta}$, *define the local multiplicity of a disk* $\widetilde{\phi}$ *at* $\widetilde{\mathbf{x}}$ *as follows. Given* $\widetilde{\phi} \in \pi_2(\widetilde{\mathbf{x}}, \widetilde{\mathbf{y}})$, *there are four regions in* $\mathbb{C} - \widetilde{\alpha} - \widetilde{\beta}$ *which contain* $\widetilde{\mathbf{x}}$ *as a corner point. Choosing interior points* $z_1, ..., z_4$ *in these four regions, define*

$$\overline{n}_{\widetilde{\mathbf{x}}}(\widetilde{\phi}) = \frac{n_{z_1}(\widetilde{\phi}) + n_{z_2}(\widetilde{\phi}) + n_{z_3}(\widetilde{\phi}) + n_{z_4}(\widetilde{\phi})}{4}. \tag{2.4}$$

     We define $\overline{n}_{\widetilde{\mathbf{y}}}(\widetilde{\phi})$ *similarly, only now choosing the points in the four regions which have* $\widetilde{\mathbf{y}}$ *as a corner point.*

   - *let the index of a disk* $\widetilde{\phi} \in \pi_2(\widetilde{\mathbf{x}}, \widetilde{\mathbf{y}})$ *be given by:*

$$\mu(\widetilde{\phi}) = 2(\overline{n}_{\widetilde{\mathbf{x}}}(\widetilde{\phi}) + \overline{n}_{\widetilde{\mathbf{y}}}(\widetilde{\phi})).$$

   - *The differential is then given by summing over disks with index one:*

$$\partial \widetilde{\mathbf{x}} = \sum_{\widetilde{\mathbf{y}}} \sum_{\{\widetilde{\phi} \in \pi_2(\widetilde{\mathbf{x}}, \widetilde{\mathbf{y}}) | \mu(\widetilde{\phi}) = 1\}} [\widetilde{\mathbf{y}}, i - \overline{n}_{\widetilde{\mathbf{w}}(\widetilde{\phi})}, j - \overline{n}_{\widetilde{\mathbf{z}}(\widetilde{\phi})}].$$

In [OS08] it is proven that this this is indeed a chain complex and that it is

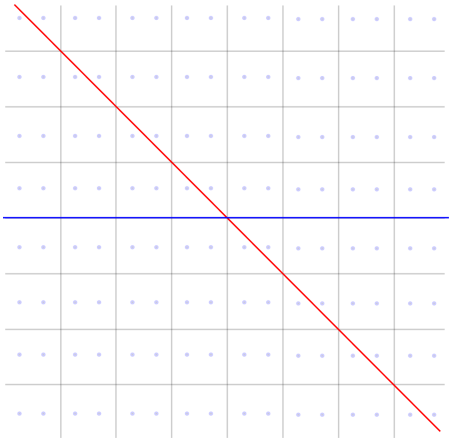

Figure 2.3: $\overline{\mathcal{H}}$ of the unknot.

chain homotopic to $CFK^\infty(\mathcal{H}(K))$.

Proposition 2.1.3 *$CFK^\infty\left(\overline{\mathcal{H}(K)}\right)$ is a chain complex and we have a filtered chain homotopy equivalence:*

$$CFK^\infty\left(\overline{\mathcal{H}(K)}\right) = CFK^\infty(\mathcal{H}(K)).$$

Proof. This is shown in [OS04a, Lemma 6.5, Proposition 6.4] □

Example 2.1.4 *Let $\widetilde{\alpha} \subset \mathbb{R}^2$ be $y + x = 0$ and $Im(\widetilde{\beta})$ be $y = 0$. Then $\overline{\mathcal{H}(K)}$ is a lifted diagram for the unknot (Figure 2.3).*

Chapter 3

Chain Complex

3.1 Reduction to Knot Surgery

$-\partial W_n$ is a surgery on a two bridge link. Instead of calculating the Floer homology of $-\partial W_n$, we focus on an associated three-manifold Y^n, which is given by surgery on a knot, K^n. The topology of Y^n is similar enough to $-\partial W_n$ that they have isomorphic Floer homology (proposition 3.1.2). Since Y^n is given by a knot surgery, we can compute $HF^+(Y^n)$ with the formula for integer surgery discovered in [OS08].

Definition 3.1.1 *Let (S^3, L^n) be the underlying link in the Kirby diagram for $-\partial W_n$. Since each of the components of L^n is individually unknotted, ± 1 surgery gives back S^3. We define a knot (S^3, K^n) by blowing down one of the components by -1 surgery (Figure 3.1). (We don't need to specify the component we are blowing down as L^n is symmetric).*

Let Y^n be the three-manifold given by $+1$ surgery on K^n. Note Y^n is also given by the kirby diagram L^n with framings $(0, -1)$.

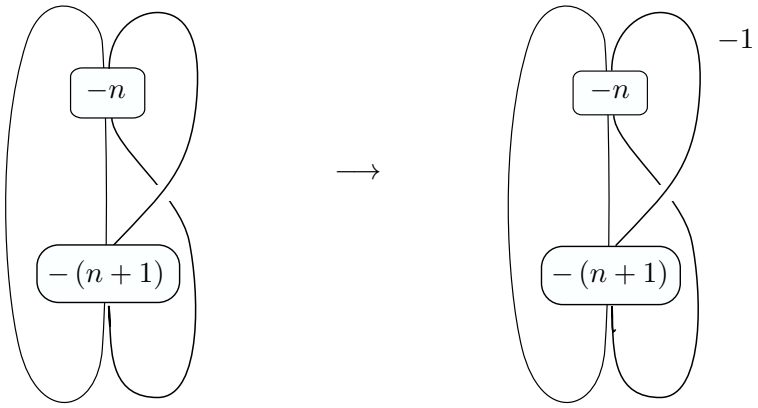

Figure 3.1: Changing a link into a knot in S^3.

Proposition 3.1.2 *There is a graded U-isomorphism between the Floer Homologies of $-\partial W_1$ and a homology sphere given by $+1$ surgery on the knot in S^3.*

$$HF^+(-\partial W_n) \cong HF^+(Y^n)$$

Proof. Y^n fits into $+1$ surgery exact sequence with $-\partial W_n$ (Figure 3.2).

Since $-\partial W_n$ an Y^n are integral homology three-spheres, they have a well defined d-invariant [OS03] as well as the splitting $HF^+ \cong \mathcal{T}^+_{(d)} \oplus HF_{red}$.

The d-invariant is zero since they bound contractible four-manifolds (for Y^n this can also be seen directly from the computations below) so they can only differ on HF_{red}. The claim will follow if we show $\partial_* : HF^+_{red}(-\partial W_n) \to HF^+_{red}(Y^n)$ is a U-module isomorphism.

The surgery exact sequence for $+1$ surgery on a homology sphere gives us:

$$\ldots \xrightarrow{\partial_*} HF^+(-\partial W_n) \xrightarrow[\frac{-1}{2}]{f_*} \mathcal{T}^+_{\frac{1}{2}} \oplus \mathcal{T}^+_{\frac{-1}{2}} \xrightarrow[\frac{-1}{2}]{g_*} HF^+(Y^n) \xrightarrow{\partial_*} \ldots \tag{3.1}$$

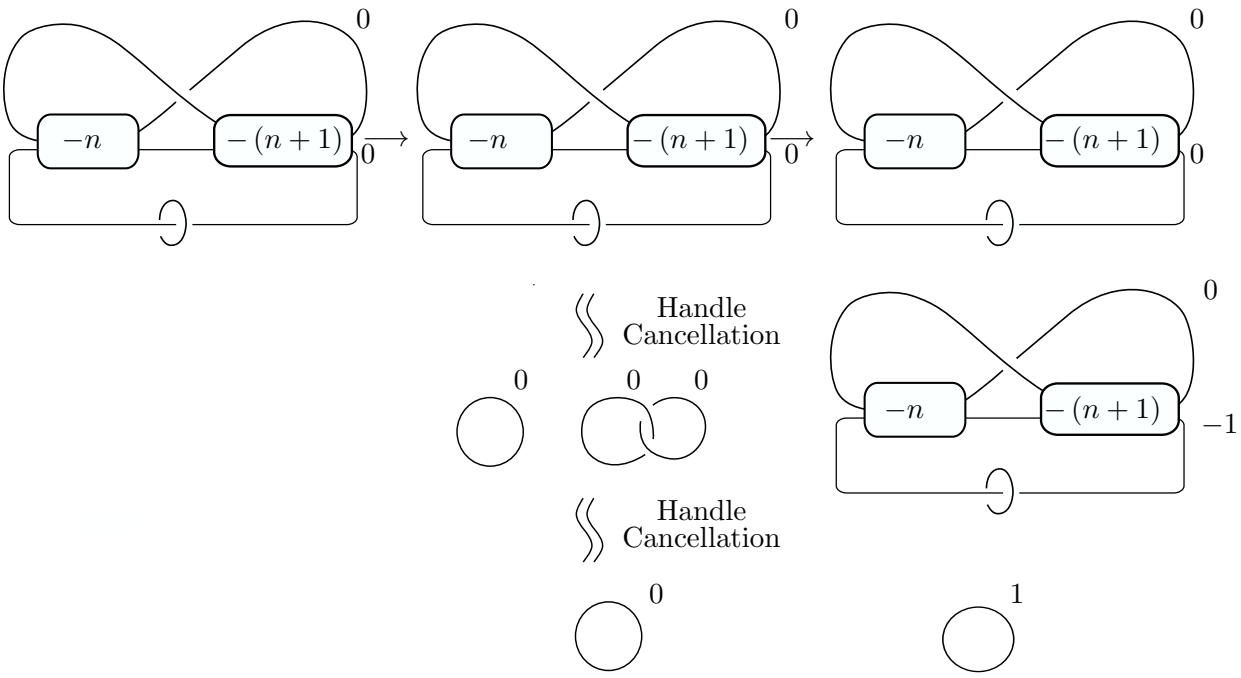

Figure 3.2: From left to right we have $-\partial W_n$, $S^1 \times S^2$, and then Y^n.

Since the Floer homology of $S^1 \times S^2$ is supported entirely in its torsion spin^c structure, the cobordism maps f_* and g_* are homogeneous of degree $\frac{-1}{2}$.

Since there is only a single $\mathcal{T}^+$ in $HF^+(-\partial W_n)$, f_* cannot be surjective and thus the cokernel of f_* will contain a subcomplex isomorphic to a $\mathcal{T}^+$. Thus the image of g_* must contain at least one subcomplex isomorphic to $\mathcal{T}^+$. This implies that the coker(g_*) and thus the image of ∂_* is finitely generated. Going back to f_*, this shows f_* is non-zero on $\mathcal{T}_0^+ \subset HF^+(-\partial W_n)$.

Let $\mathbf{x} \in \mathcal{T}_0^+ \subset HF^+(-\partial W_n)$ such that $f_*(\mathbf{x}) \neq 0$. Then let k be such that $U^k \cdot f_*(\mathbf{x}) \neq 0$ but $U^{k+1} f_*(\mathbf{x}) = 0$. Since f_* is U-equivariant, $U^k \cdot \mathbf{x} \neq 0$. Since f_* maps into $\mathcal{T}^+_{\frac{1}{2}} \oplus \mathcal{T}^+_{\frac{-1}{2}}$, the degree of $U^k \cdot f_*(\mathbf{x})$ is either $\frac{1}{2}$ or $\frac{-1}{2}$.

f_* drops degree by $\frac{1}{2}$, so $\deg\big(U^k \cdot \mathbf{x}\big) = 1$ or 0. Since $\mathcal{T}_0^+$ takes only even values, $\deg\big(U^k \cdot \mathbf{x}\big) = 0$. This shows that f_* is injective on $\mathcal{T}_0^+ \subset HF^+(-\partial W_n)$.

Since f_* is injective on $\mathcal{T}_0^+ \subset HF^+(-\partial W_n)$, we know that the $\ker(g_*) \subset \mathcal{T}_{\frac{1}{2}}$ and thus $\mathrm{Im}(g_*) \subset \mathcal{T}_0^+ \subset HF^+(-\partial W_n)$. Let $\mathbf{x}$ be the element with minimum degree in $\mathrm{coker}(f_*)$. If $\deg(\mathbf{x}) > \frac{1}{2}$, then $\deg(g_*(\mathbf{x})) > 0$. Since the d-invariant of $HF^+(Y^n) = 0$, $U \cdot g_*(\mathbf{x}) \neq 0$. This gives the contradiction:

$$0 = g_*(0) = g_*(U \cdot \mathbf{x}) = U \cdot g_*(\mathbf{x}) \neq 0.$$

Thus $\deg(\mathbf{x}) = \frac{1}{2}$ and g_* is injective on $\mathcal{T}_{\frac{1}{2}}^+ \subset HF^+(S^1 \times S^2)$. So $\mathrm{coker}(g_*) = HF_{red}(Y^n)$ and $\ker(f_*) = HF_{red}(Y^n)$. i.e. ∂_* is an isomorphism between the HF_{red} groups of the two manifolds. □

Remark 3.1.3 *In [AK12, Proposition 1.2] a more general but weaker, in the context of gradings, statement is proven. They show that there is an isomorphism $HF_{red}(Y)$ and $HF_{red}(Y_p)$ for any p. However, the isomorphism only preserves gradings for the case $p = 1$ so the Floer groups of the plumbed manifolds in their paper while isomorphic to $-\partial W_n$ for all n, only give information about the absolute gradings for $n = 1$.*

3.2 Heegaard Diagram

[OS04a] shows how to construct $\overline{\mathcal{H}(K)}$ when K is the result of blowing down one of the components of a two bridge link. The following is a formalization of their algorithm:

Notation 3.2.1 *Let sgn(i)* $= \begin{cases} +1 & i > 0 \\ -1 & i < 0 \end{cases}$

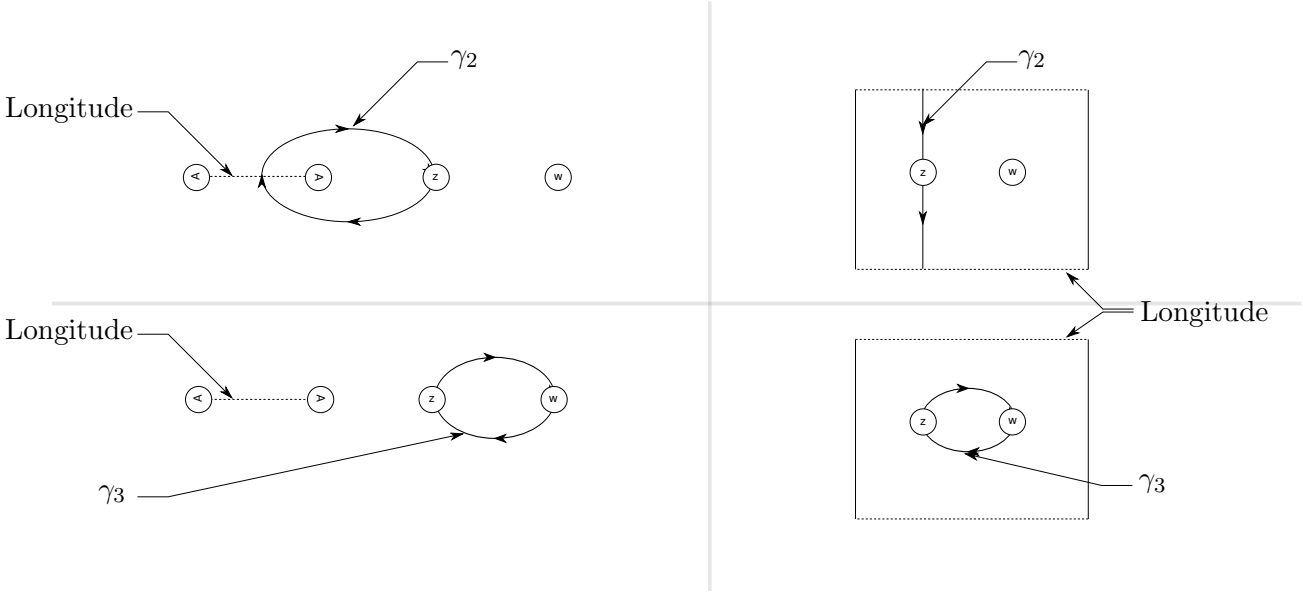

Figure 3.3: Comparison of the action on the torus: $(\psi, \mathcal{H}(K))$ (left side) To the action on the fundamental domain of the cover, $\left(\overline{\psi}, \overline{\mathcal{H}(K)}\right)$ (right side). The rotated A's denote one handles. The top row corresponds to τ_2^2. The bottom row to τ_3.

Definition 3.2.2 *Define two actions on these lifted Heegaard Diagrams (see Figure 3.3):*

- *Rotation by π: On each image of $D \subset \overline{\mathcal{H}(K)}$, perform a half Dehn twist along a circle containing both marked points.*
- *Finger move of length k: $\overline{\mathcal{H}(K)}$ along the vertical lines $\{x = n + \frac{2}{3} | n \in \mathbb{Z}\}$. Start at an intersection point of $\widetilde{\beta}$ and one of the vertical lines $\gamma \in \{x = n + \frac{2}{3} | n \in \mathbb{Z}\}$, isotope $\widetilde{\beta}$ upward (or downward, if $sgn(n) = -1$) along γ such that $\widetilde{\beta}$ crosses exactly the first $|n|$ marked points ($\widetilde{\mathbf{z}}$ or $\widetilde{\mathbf{w}}$) on γ.*

$\overline{\mathcal{H}(K)}$ can be obtained by repeated applications of the above two moves:

Lemma 3.2.3 *Let K be obtained by blowing down a component of a two bridge link L.*

Let σ be an element of the braid group on four strands whose plat closure is the two bridge link, $\overline{\sigma} = L$.

Factor σ into the generating set $\{\tau_i\}_{i=1,2,3}$, where τ_i gives a positive crossing to the strands i and $i+1$.

If we blowdown with a -1 surgery, start with the lifted Heegaard Diagram for an unknot, $\overline{\mathcal{H}(K)}$, given in example 2.1.4. For a $+1$ framed blowdown, let $Im(\widetilde{\beta}) = \{y - x = 0\}$ instead.

Proceeding from left to right along the braid word obtained by factoring $\overline{\sigma}$, we apply vertical shifts or rotations according to the following identifications:

- τ_2^{-2n} *or* $\tau_2^{2n} \leftrightarrow$ *finger move of length* $-n$ *or* $+n$.
- τ_3^{-1} *or* $\tau_3 \leftrightarrow$ *rotation by* π *or* $-\pi$.

Proof. [OS04a, Proposition 6.3] proves this for the $\mathcal{H}(K)$. In particular, they show, for $\gamma_{1,2}$ in Figure 3.3, that:

- $\tau_1^{-2n} = \tau_2^{2n} \leftrightarrow$ Full Dehn twist along the circle γ_1
- $\tau_3 \leftrightarrow$ Half Dehn twist along the circle γ_3

To see it for $\overline{\mathcal{H}}$, we check that it commutes with the covering map π:

$$\begin{array}{ccc} \overline{\mathcal{H}(K)} & \xrightarrow{\overline{\psi}} & \overline{\mathcal{H}(K)} \\ \downarrow & \circlearrowleft & \downarrow \\ \mathcal{H}(K) & \xrightarrow{\psi} & \mathcal{H}(K) \end{array}$$

Since the unit square D is a fundamental domain for $\overline{\mathbb{R}^2}$, $\overline{\psi}$ is determined by its restriction to D.

The support of the half Dehn twist, ψ_3 induced by τ_3 doesn't intersect the boundary of the fundamental domain D so the lift $\overline{\psi_3}|_D$ is still a half Dehn twist. (Bottom right of Figure 3.3). The full Dehn twist, ψ_1 induced by $\tau_1^{-2n} \leftrightarrow \tau_2^{2n}$ unwinds to become a linear push on the cover as ψ_1's support is a neighborhood of the circle γ_3, which lifts to $\mathbb{R} \subset \overline{\mathbb{R}^2}$ (Top right of Figure 3.3).

□

Corollary 3.2.4 *$CFK^\infty(S^3, K^n)$ is chain homotopic to the combinatorial chain complex associated to the Heegaard Diagram $\overline{\mathcal{H}(K^n)}$ (Figure 3.4).*

Proof. L^n factors into the braid word $\tau_1^{-2n} \circ \tau_2 \circ \tau_1^{-2(n+1)}$. Following lemma 3.2.3, we begin with Figure 2.3 and apply the sequence of moves:

- τ_1^{-2n} corresponds to making a finger of length $-n$
- The τ_2 is a rotation by π which transforms the single long finger, created by the previous move, into n pairs of fingers.
- $\tau_1^{-2(n+1)}$, a finger move of length $-n-1$, stretches the $2n$ fingers to a length of $n+1$.

(see Figure 3.5).

□

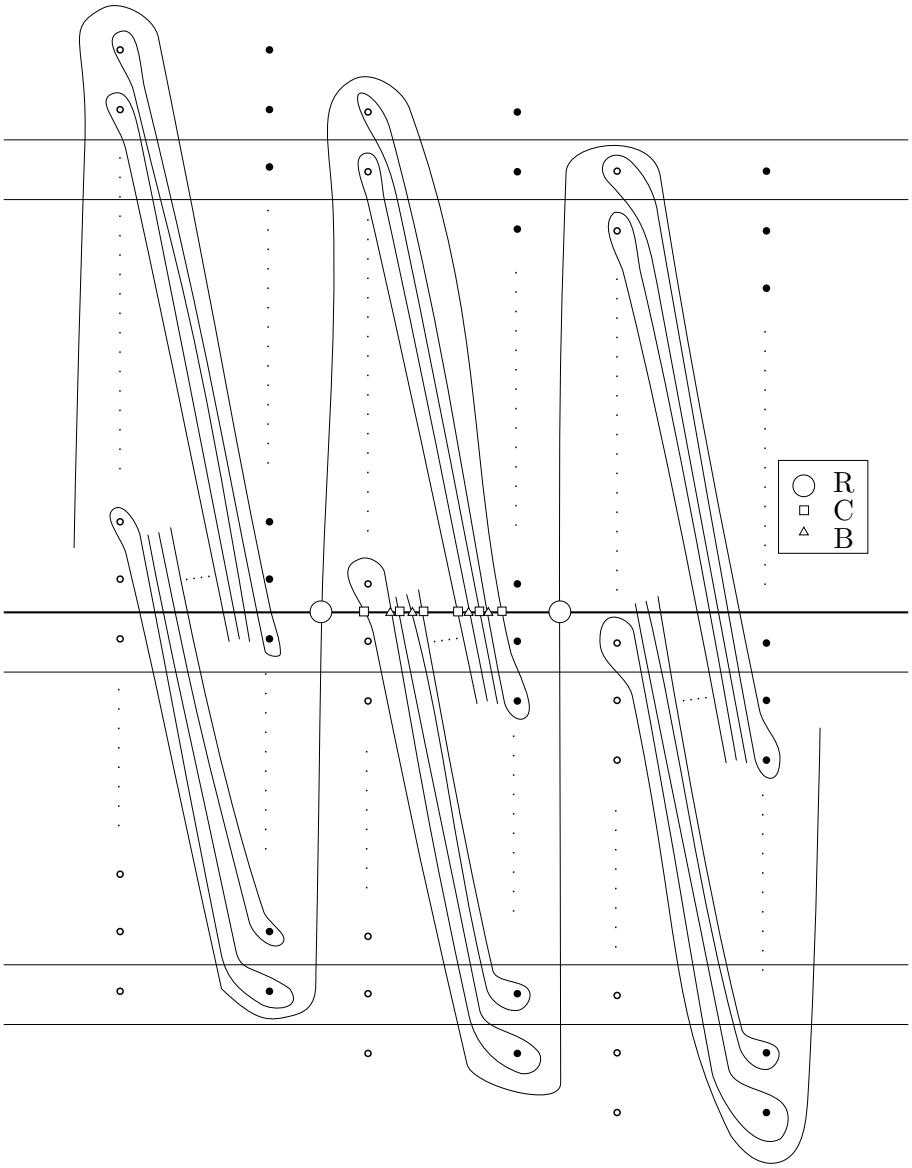

Figure 3.4: $\overline{\mathcal{H}(K^n)}$. See Figure 3.14 for an example when $n = 2$. The label B is used for points that will function as *boundaries* in the homology computation. Likewise, R for *relations* and C for *generators*

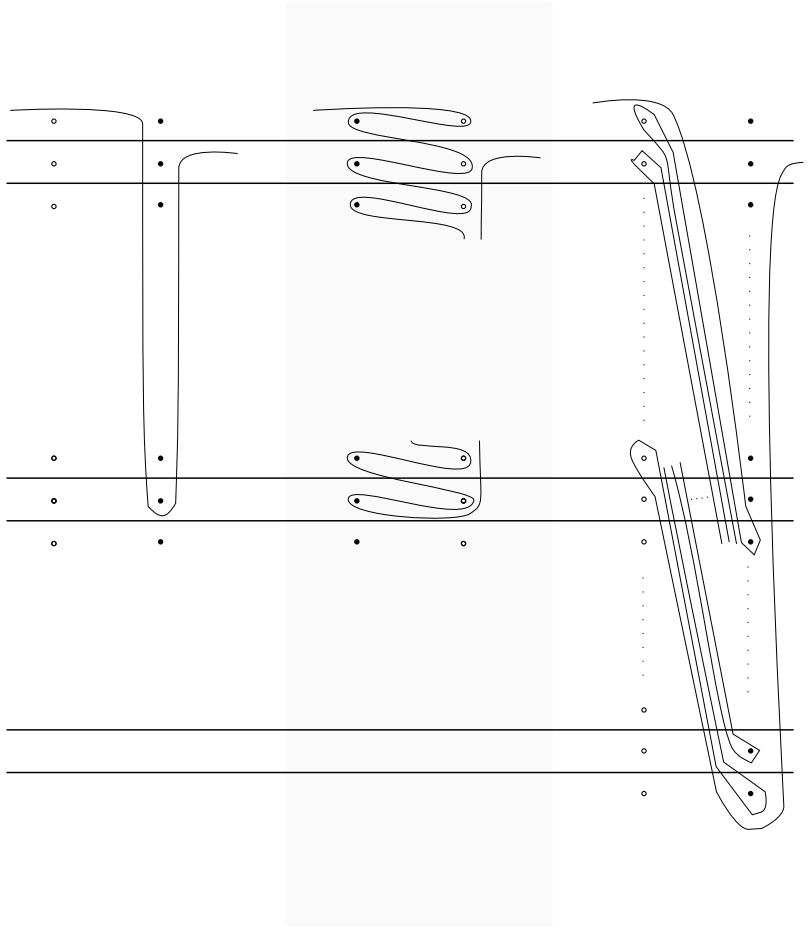

Figure 3.5: $\tau_1^{-2n} \to \tau_2 \to \tau_1^{-2(n+1)}$.

3.3 Chain Complex

Recall that

$$CFK^\infty \cong \mathbb{F}[U, U^{-1}] \otimes \mathcal{R}.$$

We prove several propositions about $\mathcal{R}$ and combine them at the end of the section to get CFK^∞ in Theorem 3.3.14.

Abusing notation, the elements of $\widetilde{\alpha} \cap \widetilde{\beta}$ as well as the elements they correspond to in chain complex $\mathcal{R}$ will be denoted by the same symbol. This does

not cause any difficulties as the coefficients are in $\mathbb{F} = \mathbb{Z}/2\mathbb{Z}$.

Notation 3.3.1 *Let $\langle A \rangle$ denote the free module over A with coefficients in $\mathbb{F}$*

In figure 3.4, $\widetilde{\alpha} \cap \widetilde{\beta}$ was split into three sets: R, C and B foreshadowing their roles as the *Relations, Cycles, and Boundaries* of $\mathcal{R}$. A precise definition of R, C and B:

Definition 3.3.2 *Partition $\widetilde{\alpha} \cap \widetilde{\beta}$ into three classes R, C, and B:*

1. *An element $\widetilde{\mathbf{x}} \in \widetilde{\alpha} \cap \widetilde{\beta}$ has four regions, in $\overline{\mathcal{H}(K^n)} - \left(\widetilde{\alpha} \cup \widetilde{\beta}\right)$, that have $\widetilde{\mathbf{x}}$ as a corner. If two or more of these regions are not compact,*

$$\widetilde{\mathbf{x}} \in R$$

Enumerate R:

$$R = \{r_{-(n-1)}, ..., r_0, ..., r_{(n-1)}\}$$

2. *Put an orientation on $\widetilde{\alpha}$ and $\widetilde{\beta}$ that makes at least one intersection point $r \in R \subset \widetilde{\alpha} \cap \widetilde{\beta}$ have a positive sign. (In fact all $r \in R$ have the same sign).*

   $\widetilde{\mathbf{x}} \in B$ (respectively C) if $\widetilde{\mathbf{x}}$ has positive (negative) sign with the orientation.

3. *Let S_i be the subset of $\left(\widetilde{\mathbb{T}}_\alpha \cap \widetilde{\mathbb{T}}_\beta\right)$ which lie on $\widetilde{\alpha}$ between r_i and $r_{i+sgn(i)}$, $i \neq 0$. For $i = 0$, Let S_{0^-} be the subset between r_{-1} and r_0 and S_{0^+} be the subset between r_0 and r_1.*

The awkward notation of $S_{0^{\pm 1}}$ is used to highlight the identification of the r_i with S_i.

Denote $C_i = S_i \cap C$ and $B_i = S_i \cap B$

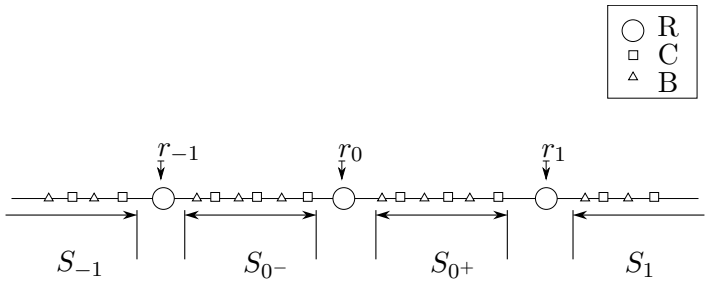

Figure 3.6: A classification of the intersection points on $\widetilde{\alpha} \cap \widetilde{\beta}$

Lemma 3.3.3

$$\mu(b) + 1 = \mu(g) = \mu(r) - 1$$

$\forall \quad b \in B, g \in C, r \in R$

Proof. Within a particular S_i the alternating upward and downward *fingers* show the alternating g and b points to be split into two Maslov degrees.

The two compact domains (the other two are always non compact) with a corner at a given r_i can be completed by adding fingers to form a Maslov index one bigon to the two adjacent (along $\widetilde{\alpha}$) points in R (Figure 3.12). This shows the g, and thus also the b of different S_i and r_i, to have (respectively) the same relative Maslov degree. □

The difficult part in computations of CFK^∞ is generally the differential. For 'lifted' diagrams $\overline{\mathcal{H}}$, [OS04a, section 6.2]. shows the differentials can be computed combinatorially. It particular, if $\widetilde{\phi} \in \pi_2(\widetilde{\mathbf{x}}, \widetilde{\mathbf{y}})$ with $\mu(\widetilde{\phi}) = 1$:

- $\widetilde{\phi}$ is unique and a bigon. (Follows from genus being one.)
- $\#\widehat{\mathcal{M}}(\widetilde{\phi}) = 1 \Leftrightarrow \mathcal{D}(\widetilde{\phi}) \geq 0$ [OS04a, proposition 6.4]
- $\overline{n}_{\widetilde{\mathbf{x}}} = \frac{1}{4} = \overline{n}_{\widetilde{\mathbf{y}}}$ [OS04a, proposition 6.5]

Proposition 3.3.4 *The differential respects the S_i:*

1. *For $r_i \in R$, $\partial r_i \in \left\langle S_{i+sgn(i)} \cup S_i \right\rangle$*
2. *If $\widetilde{\mathbf{x}} \in \langle S_i \rangle$, $\partial\widetilde{\mathbf{x}} \in \langle S_i \rangle$*

Proof. This follows from the inability of positive bigons to cross the points $\{r_{-(n-1)}, ..., r_0, ..., r_{(n-1)}\}$. Suppose a bigon has an r_i on its boundary, $r_i \in \partial\widetilde{\phi}$. Then r_i must be a *corner* of $\widetilde{\phi}$. i.e. $r_i = \widetilde{\mathbf{x}}$ or $\widetilde{\mathbf{y}}$ where $\widetilde{\phi} \in \pi_2(\widetilde{\mathbf{x}}, \widetilde{\mathbf{y}})$

Inspecting the diagram, we see that for every $r_i \in R$ there are four domains which have r_i as a corner point (Figure 3.7). Since $r_i \in \partial\widetilde{\phi}$ at least one of these must have a non-zero positive coefficient in $\mathcal{D}\left(\widetilde{\phi}\right)$. Only the two of these are compact and can have a non-zero coefficient in $\mathcal{D}\left(\widetilde{\phi}\right)$. Since the two compact domains are oppositely oriented with respect to the $\widetilde{\alpha}$ and $\widetilde{\beta}$ curves, their coefficients in $\mathcal{D}\left(\widetilde{\phi}\right)$ must have opposite signs. As we are only interested in $\mathcal{D}\left(\widetilde{\phi}\right) \geq 0$ exactly one of the domains has a non-zero positive coefficient. □

Definition 3.3.5 *The two compact domains of Figure 3.7 with corners at r_i, will be called* gloves. *The name was chosen to fit in with the following definitions of* fingers *domains and* palm *domains.*

Lemma 3.3.6 *For a given S_i, there are only two domains out of which all of the other $\mathcal{D}\left(\widetilde{\phi}\right)$ with $\mu\left(\widetilde{\phi}\right) = 1$ are composed:*

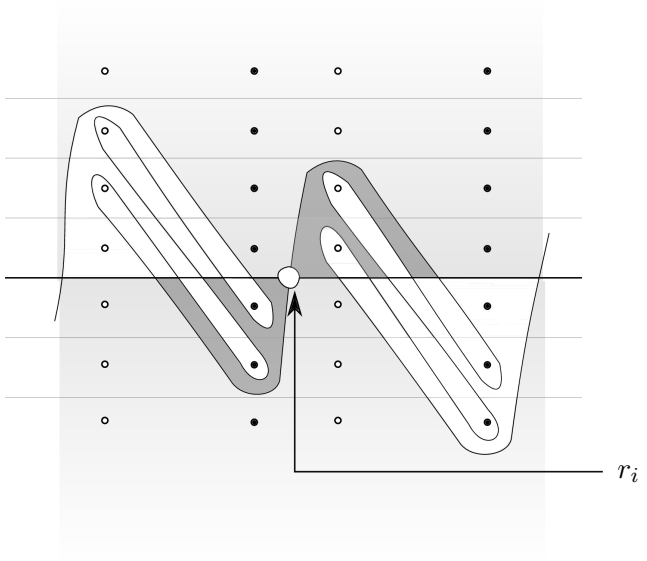

Figure 3.7: Four domains with a corner at r_i. The two compact domains are darkly shaded. The two non-compact domains are lightly shaded.

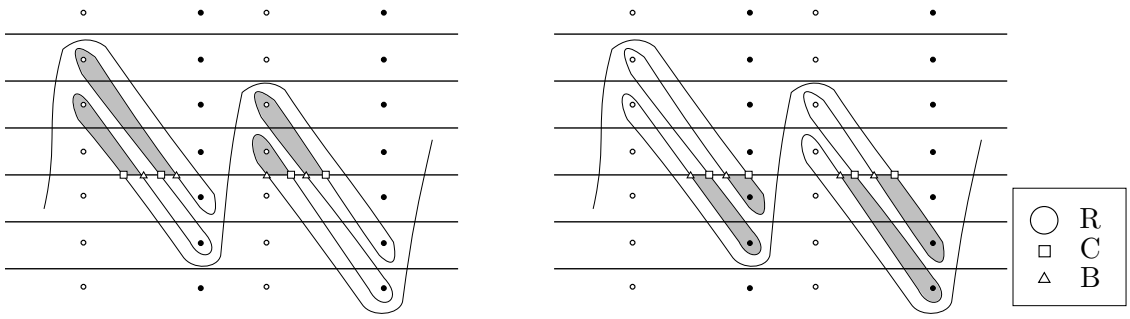

Figure 3.8: *Upward pointing fingers* on the left and *downward pointing fingers* on the right

1. Fingers *with a corners at adjacent $c \in C$ and $b \in B$ (Figure 3.8).*

2. Palms *Bigons with one corner in R and the other corner at the $c \in C$ which precedes the next element of R (Figure 3.9),*

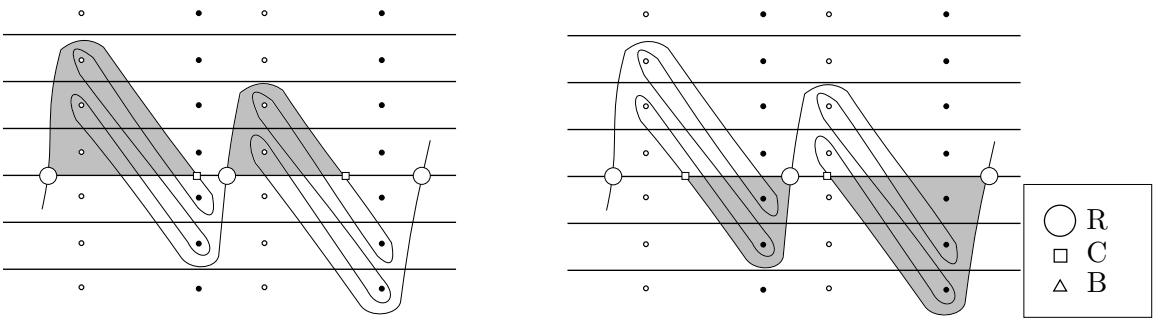

Figure 3.9: *Upward pointing Palms* on the left and *downward pointing Palms* on the right

Definition 3.3.7 *The union of a all of the upward* fingers *and the downward* palm *will be called, of course, an upward* hand. *Likewise for a downward* hand.

Proof. (lemma 3.3.6) It suffices to prove this for *fingers* and *gloves* instead - By adding and removing *fingers*, we can construct *palms* from *gloves* and vice versa. Thus together with the *finger* domains, they generate the same set of domains $\mathcal{D}\left(\widetilde{\phi}\right)$:

$$\langle palms, fingers\rangle \Leftrightarrow \langle gloves, fingers\rangle$$

Clearly if $\mathcal{D}\left(\widetilde{\phi}\right) \in \langle gloves, fingers\rangle$ then $\mathcal{D}\left(\widetilde{\phi}\right) \in S_i$. (i.e. $\widetilde{\mathbf{x}}, \widetilde{\mathbf{y}} \in S_i$). On the other hand, if $\mathcal{D}\left(\widetilde{\phi}\right)$ is compact but $\notin \langle gloves, fingers\rangle$ then it must pass contain one of the *gloves* of proposition 3.3.6. Otherwise $\mathcal{D}\left(\widetilde{\phi}\right)$ would have

more than one connected component and have a Maslov index greater than one. However proposition 3.3.6 concluded that this isn't possible. □

We introduce some simple chain complexes commonly referred to as *rails*. [OS04b]. In [OS04b, Theorem 12.1], they showed $\widehat{CFL}$ could be given a simple description as a direct sum of *rails* and some other simple complexes. Unfortunately, CFK^∞ does not have as simple of a description, but the *rails* nonetheless allow a construction of a tractable complex.

Definition 3.3.8 *A rail is an indecomposable bigraded chain complex with elements* $\{x_{2i}, y_{2i\pm1}\}_{a\leq 2i, 2i\pm1\leq b}$, $a, b \in \mathbb{Z}$, *with differentials:*

$$\partial y_{2i\pm1} = 0$$

and

$$\partial x_{2i} = y_{2i-1} + y_{2i+1}$$

(If either y_{2i-1} *or* y_{2i+1} *don't exist replace them with* 0 *in the above differential). The relative filtration levels between* x_{2i} *and* y_{2i-1}, y_{2i+1} *are given by:* $\mathcal{F}(x_{2i}, y_{2i-1}) = (1, 0)$ $\mathcal{F}(x_{2i}, y_{2i+1}) = (0, 1)$.

The length of the rail is $max(\#\{x_{2i}\}, \#\{y_{2i\pm1}\})$.

Remark 3.3.9 *A rail has homology* $\mathbb{F}$ *if* $\#\{x_{2i}, y_{2i\pm1}\}_{a\leq 2i, 2i\pm1\leq b}$ *is odd and is acyclic otherwise. See the right hand side of figure 3.10 for an example.*

As a first application of Lemma 3.3.6, we show there is a *rail* induced by each S_i.

Proposition 3.3.10 *$\langle c, b \in S_i \rangle$ generates a subcomplex isomorophic to a rail (see figure 3.10).*

Proof. (proposition 3.3.10) Lemma 3.3.6, immediately gives us:

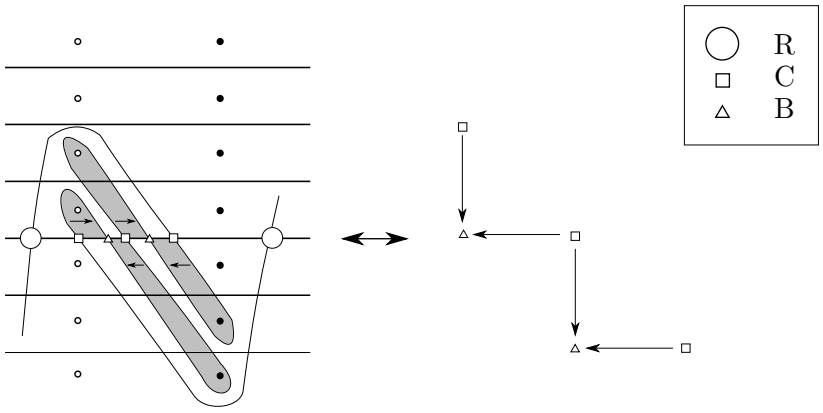

Figure 3.10: A rail of length two. The darkly shaded regions of the Heegaard Diagram are the *fingers* that induce the differentials in the chain complex on the right. The arrows inside the fingers are a visual aid denoting the direction of the differential.

$$\partial\left(S_i\right) \subset S_i.$$

Thus S_i is a subcomplex. Once again, by lemma 3.3.6, we can get away with only looking at linear combinations of fingers and palms. Since the palms have a corner in R, and S_i was explicitly defined not to contain them there are no differentials in the subcomplex S_i induced by a $\mathcal{D}\left(\widetilde{\phi}\right)$ containing a palm. This leaves only the fingers, which all contribute differentials. (Figure 3.10) $\square$

Taken by itself, the homology $H_*(S_i, \partial)$ of a single rail is $\mathbb{F}$ and is generated by the cycle $\sum_{c \in C_i} c$. The missing elements and differentials, (R, ∂), have the effect of equating these cycles.

Proposition 3.3.11

$$\partial r_i = \sum_{c \in C_i \cup C_{i+sgn(i)}} c$$

If either S_i or $S_{i+\mathrm{sgn}(i)}$ does not exist, take it to be $\varnothing$.

Proof. The argument is very similar to the previous proof. Corollary 3.3 together with the Maslov index, lemma 3.3.3 show:

$$\partial r_i \subset \left\langle C_i \cup C_{i+\mathrm{sgn}(i)} \right\rangle .$$

We can make this an equality by explicitly constructing bigons. Start with a palm and successively add pairs of upward and downward fingers (Figure 3.11). The pairs must be adjacent for the Maslov count to be unchanged.

□

Lemma 3.3.6 tells us that all of the domains contributing differentials to the subcomplex $\langle S_i \rangle$ are within the vertical strip bounded by the lines perpendicular to r_i and r_{i+1} (Figure 3.14).

Lemma 3.3.12 *There are two* gloves *having a given S_i as a border. The upward pointing hand $\widetilde{\phi}$ has:*

$$\begin{aligned} n_{\widetilde{\mathbf{z}}}(\widetilde{\phi}) &= 0 \\ n_{\widetilde{\mathbf{w}}}(\widetilde{\phi}) &= \max(0, -i) \end{aligned}$$

If $\widetilde{\phi}$ is pointing downward:

$$\begin{aligned} n_{\widetilde{\mathbf{z}}}(\widetilde{\phi}) &= \max(0, i) \\ n_{\widetilde{\mathbf{w}}}(\widetilde{\phi}) &= 0 \end{aligned}$$

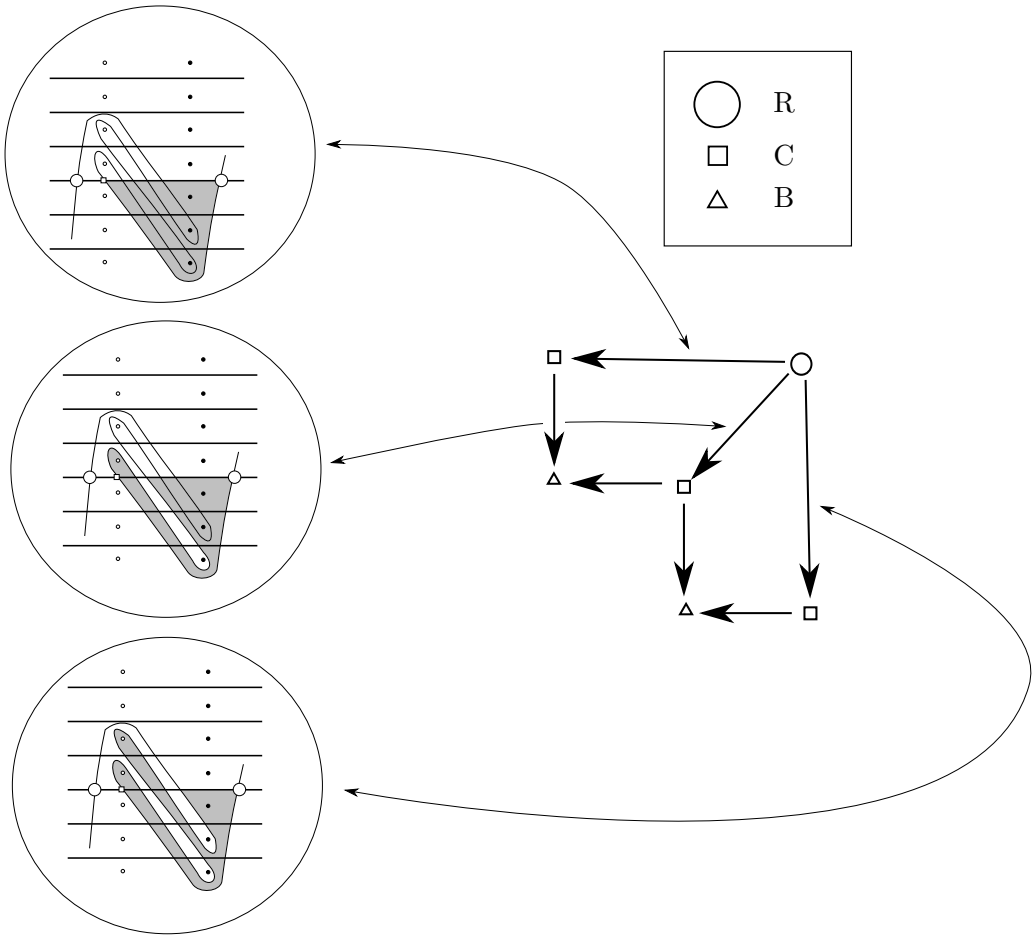

Figure 3.11: Compare with Figure 3.10

Proof. By inspection of figure 3.4. Counting the upward pointing hands:

1. The upward *hands* lying above $\{S_i\}_{i>0}$ have $n_{\widetilde{\mathbf{z}}}(\widetilde{\phi}) = 0$ and $n_{\widetilde{\mathbf{w}}}(\widetilde{\phi}) = 0$.

2. The upward *hands* lying above $\{S_i\}_{i<0}$ have $n_{\widetilde{\mathbf{z}}}(\widetilde{\phi}) = 0$ but $n_{\widetilde{\mathbf{w}}}(\widetilde{\phi}) = |i|$

Analogously for downward pointing *hands*:

1. The downward *hands* lying below $\{S_i\}_{i<0}$ have $n_{\widetilde{\mathbf{z}}}(\widetilde{\phi}) = 0$ and $n_{\widetilde{\mathbf{w}}}(\widetilde{\phi}) = 0$.

2. The downward *hands* lying below $\{S_i\}_{i>0}$ have $n_{\widetilde{\mathbf{w}}}(\widetilde{\phi}) = 0$ but $n_{\widetilde{\mathbf{z}}}(\widetilde{\phi}) = i$

□

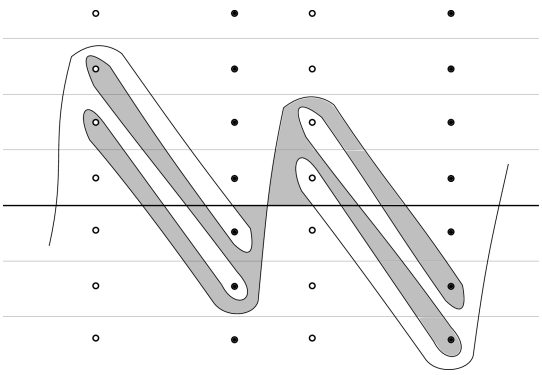

Figure 3.12: The shaded region on the left is an upward hand, the shaded region on the right is a downward hand.

Proposition 3.3.13 $\mathcal{F}(r_{i+1}, r_i) = (i, i+1)$

Proof. Since the diagram is invariant when rotated by π and switching $\widetilde{\mathbf{z}} \leftrightarrow \widetilde{\mathbf{w}}$, it suffices to prove the result for $\{r_i | i \geq 0\}$.

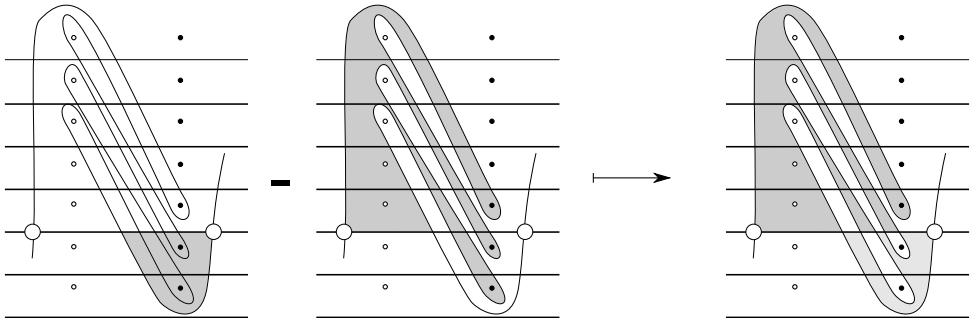

Figure 3.13: A vertical strip in the diagram for Y^3 between r_1 and r_2. The left domain is $\widetilde{\phi}$. The middle, $\widetilde{\psi}_i$ The right is their difference $\widetilde{\phi}_i - \widetilde{\psi}_i$. The lighter shaded region is negative.

The relative filtration levels between r_i and r_{i+1} is calculated with the domain given by (Figure 3.13):

$$\widetilde{\phi}_i - \widetilde{\psi}_i$$

By inspection, all but i of the *fingers* cancel each other out. Giving us: $|\{n_{\widetilde{\mathbf{z}}}\}| = i$. Lemma 3.3.12 tells us the upper *glove* contributes nothing and the lower has $|\{n_{\widetilde{\mathbf{w}}}\}| = i + 1$.

Thus we have:

$$\mathcal{F}_1(r_i, r_{i+1}) = -i$$

$$\mathcal{F}_2(r_i, r_{i+1}) = -(i+1)$$

$$\mathcal{F}_1(r_i, r_{i-1}) = -(i+1)$$

$$\mathcal{F}_2(r_i, r_{i-1}) = -i$$

□

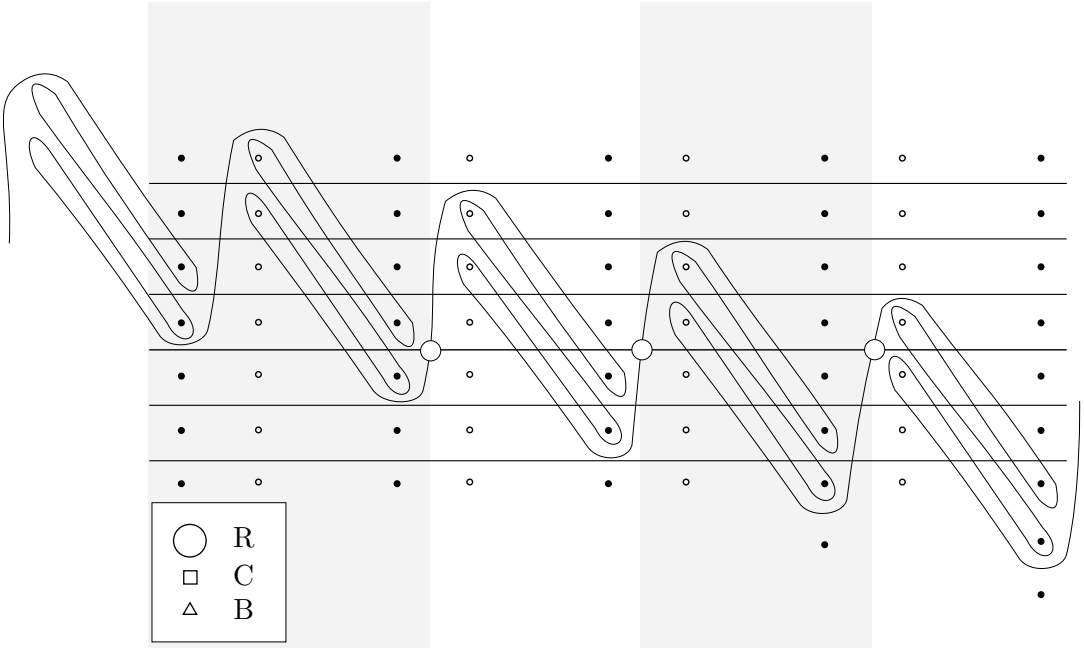

Figure 3.14: The alternating stripes distinguish four *hands* for the diagram $\overline{\mathcal{H}(K^2)}$. See figure 3.14 for its associated chain complex $CFK^\infty\left(\overline{\mathcal{H}(K^2)}\right)$.

We summarize this sections calculations and give CFK^∞ an absolute grad-

ing:

Theorem 3.3.14 *The filtered chain complex* $CFK^\infty\left(\overline{\mathcal{H}(K^n)}\right)$ *is given by* $\mathbb{F}[U,U^{-1}]\otimes\mathcal{R}$ *where* $\mathcal{R}$ *is a chain group generated over* $\mathbb{F}$ *by the set* $R\cup C\cup B$.

Since $\mathbb{F}=\mathbb{Z}/2\mathbb{Z}$ *we can and will abuse notation by identifying the intersection points* $R\cup C\cup B$ *with the algebraic elements they induce in* $\mathcal{R}$. $\mathcal{R}$ *is then just the chain complex generated from the intersection points in the diagram with differentials corresponding to the Whitney disks. See figure 3.15 for an example.*

1. *The differentials are*

   - $\partial r_i=\sum_{c\in C_i\cup C_{i+sgn(i)}} c$

     For $i=0$, $\partial r_0=\sum_{c\in C_{0^-}\cup C_{0^+}} c$

     If either S_i *or* $S_{i+sgn(i)}$ *does not exist, take it to be* $\varnothing$.

   - *The differentials of the* c *and* b *are best understood graphically. They form a rail 3.3.8 with* c *denoting the higher grading generators.*

2. *The filtration levels are:*

   - *for* $r_i\in R$:
   $$\mathcal{F}(r_i)=\left(\frac{i^2-i}{2},\frac{i^2+i}{2}\right)$$

   - *The* $c,b\in S_i$, *form a rail of length* $m=n-i$ *with filtration level stretching from* $(\frac{i^2-i}{2}-m,\frac{i^2+i}{2})$ *to* $(\frac{i^2-i}{2},\frac{i^2+i}{2}-m)$

3. *The homology is generated by any of the homologous cycles:* $[\sum_{c\in C_i} c]$

for any $-(n-1) \leq i \leq n-1$.

$$\mathbb{F} = H_*(S_i) = \left[\sum_{c \in C_i} c\right]$$

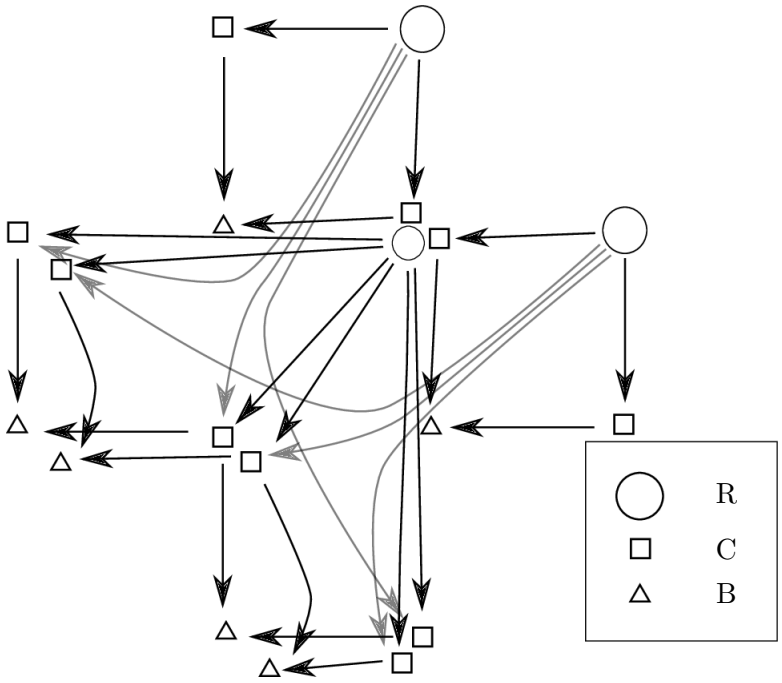

Figure 3.15: $\mathcal{R}$ for the complex $CFK^\infty\left(\overline{\mathcal{H}(K^2)}\right)$. The differentials from $r_{\pm 1}$ to the *rails* centered on r_0 are drawn curved and with a light hue. This is only to add clarity to a cluttered figure and doesn't have any mathematical significance. See figure 3.14 for the lifted Heegaard Diagram this complex is derived from.

Proof. (Theorem 3.3.14) The claim about the differentials is just a restatement of propositions 3.3.11 and 3.3.10.

The absolute grading on CFK^∞ is determined by looking at $\widehat{CFK}$ ([OS04a]). Since $H_*\left(\widehat{CF}(S^3)\right) = \mathbb{F}$, there is a unique class of cycles generating the homology. Assigning Maslov grading 0 to the image of the inclusion of these

cycles into CFK^∞, and then extending linearly gives the absolute Maslov grading.

Recall $\widehat{CF} = CFK^\infty\{i = 0\}$ and so $\mathcal{F}_1(\mathbf{x}, \mathbf{y}) = 0,\ \forall \mathbf{x}, \mathbf{y} \in \widehat{CF}$. Thus we ignore all but the completely vertical differentials in analyzing $\widehat{CF}$. We show that $\widehat{CF}$ is a direct sum of two simple subcomplexes (figure 3.16).

Figure 3.16: A cyclic and acyclic complex

For a fixed m, $U^m \otimes r_i \in \widehat{CF}$, $\partial(U^m \otimes r_i)$ now consists of only the $c \in U^m \otimes S_i$ with $\mathcal{F}_1(U^m \otimes r_i, U^m \otimes c) = 0$.

1. If $i \neq 0$, $\partial U^m \otimes r_i$ consists of exactly one element, the $U^m \otimes c$ at the bottom of a rail. Since the only differential from this $U^m \otimes c$ shifts the filtration level horizontally, the $U^m \otimes r_i$ and $U^m \otimes c = \partial(U^m \otimes r_i)$ generate an acyclic subcomplex (left figure of figure 3.16).

2. If $i = 0$, There are two rails S_{0^-}, S_{0^+} and so $\partial U^m \otimes r_i$ consists two different $U^m \otimes c$ and together they form a cyclic subcomplex (right figure of figure 3.16).

The only other differentials are those inside a rail $U^m \otimes S_i$. Since these alternate from shifting the filtration level horizonatally and vertically, their image in $\widehat{CF}$ is composed of acyclic subcomplexes (right figure of Figure 3.17).

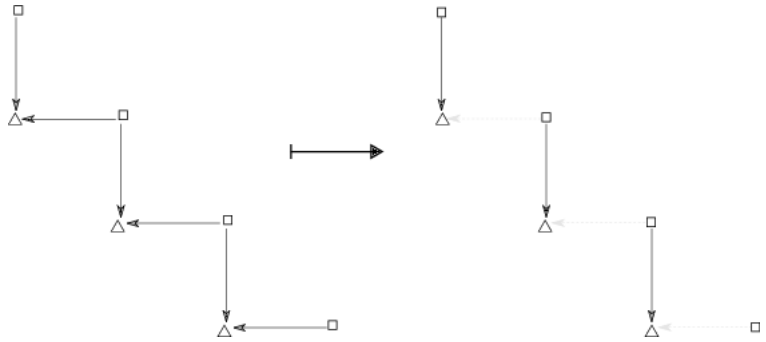

Figure 3.17: The remnants of a rail in $\widehat{HFK}$.

The homology is then generated by the subcomplex of $\widehat{CF}$ generated by $\{U^m \otimes r_0, U^m \otimes c\}$. Thus $\mathcal{F}_1(U^m \otimes c) = \mathcal{F}_1(U^m \otimes r_0) = 0$.

The symmetry of CFK^∞ then forces $\mathcal{F}_2(r_0) = 0$.

The filtration levels of the remaining r_i are given by the calculation in proposition 3.3.13 of the relative filtration levels of the r_i and the identity $\sum_{k=1}^{n} k = \frac{n(n+1)}{2}$.

The claim about the homology amounts to computing $H_*(U^m \otimes \mathcal{R})$.

Consider the subcomplex generated by the rail $U^m \otimes S_i$.

$$H_*(U^m \otimes S_i) = \left[\sum_{c \in C_i} U^m \otimes c\right] = \mathbb{F}$$

proposition 3.3.11 tells us that $\partial U^m \otimes r_i$ equates the cycles: $\sum_{c \in C_i} U^m \otimes c \sim \sum_{c \in C_{i+1}} U^m \otimes c$.

Thus the induced cycles are homologous: $\left[\sum_{c \in C_i} U^m \otimes c\right] = \left[\sum_{c \in C_j} U^m \otimes c\right]$ for all i, j.

□

Chapter 4

Integer Surgery

Definition 4.0.15 *Recall from 2.0.14:*

- $\mathcal{C}_s = \{U^m \otimes \mathbf{x} \in CFK^\infty | \mathcal{F}_1 (U^m \otimes \mathbf{x}) < 0 \text{ and } \mathcal{F}_2 (U^m \otimes \mathbf{x}) < s\}$
- $C\{i < 0\} = \{U^m \otimes \mathbf{x} \in CFK^\infty | \mathcal{F}_1 (U^m \otimes \mathbf{x}) < 0\}$.
- $A_s^+ = \frac{CFK^\infty}{\mathcal{C}_s}$
- $B_s^+ = \frac{CFK^\infty}{C\{i<0\}}$
- $\mathbb{X}^+(1)$ *is then the mapping cone of*

$$D_1^+ : \mathbb{A}^+ \longrightarrow \mathbb{B}^+$$

where

$$\mathbb{A}^+ = \bigoplus_s A_s^+$$

$$\mathbb{B}^+ = \bigoplus_s B_s^+$$

and D_1^+ is the direct sum of the chain maps:

$$D_1^+ = \bigoplus_s v_s^+ \oplus h_s^+.$$

Also, denote, by $p_s : CFK^\infty \longrightarrow \mathcal{C}_s$, the projection map.

Using the integer surgery formula [OS08], $HF^+(-\partial W_n)$ will be computed from the mapping cone $\mathbb{X}^+(1)$.

Definition 4.0.16 *For convenience, we define two small generalizations of $HF^\pm_{Red}$ for $k >> 0$:*

$$H_*^{Red}\left(A_s^+\right) = \frac{H_*\left(A_s^+\right)}{U^k \otimes H_*\left(A_s^+\right)}$$

$$H_*^{Red}\left(\mathcal{C}_s\right) = Ker\left(U^k : H_*(\mathcal{C}_s) \longrightarrow H_*(\mathcal{C}_s)\right)$$

Note, these HF_*^{Red} are defined identically to $HF^\pm_{\mathrm{red}}$. The only difference being they are defined on different subcomplexes ($\mathcal{C}_s$ vs. CF^-) and quotients (A_s^+ vs. CF^+) of CFK^∞. In particular,

1. There is a long exact sequence induced by the short exact sequence:

$$0 \longrightarrow \mathcal{C}_s \longrightarrow CFK^\infty \longrightarrow A_s^+ \longrightarrow 0.$$

2. It is also clear that they are finitely generated as they differ from CF^-, CF^+ in only finitely many elements.

Since this is all that is used to prove the isomorphism between HF^-_{red} and HF^+_{red}, [OS04d, Proposition 4.8], we can also conlude:

Proposition 4.0.17 *There is a homogeneous graded isomorphism which drops degree by 1 between $H_*^{Red}(\mathcal{C}_s)$ with $H_*^{Red}(A_s^+)$*

The computation of $H_*(\mathbb{X}(n))$ will be reduced to computing the $H_*^{\mathrm{Red}}(A_s^+)$ in proposition 4.0.21 below. $H_*^{\mathrm{Red}}(A_s^+)$ can be calculated from $H_*^{\mathrm{Red}}(\mathcal{C}_s)$ by means of an isomorphism of $H_*^{\mathrm{Red}}(\mathcal{C}_s)$ with $H_*^{\mathrm{Red}}(A_s^+)$, proposition 4.0.17. Understanding $\mathcal{C}_s$ is thus the key part of the calculation.

We investigate the structure of the chain complex $\mathcal{C}_s$ with lemma 4.0.18, show the homology of $-\partial W_n$ can be derived from it, and finish off with the calculation of the homology of $HF^+(-\partial W_n)$.

Lemma 4.0.18 *Let $p_s : CFK^\infty \longrightarrow \mathcal{C}_s$ be the projection.*

Then $\mathcal{C}_s$ is a direct sum of the U-modules (1) and (2) below.

1. *A direct sum of rails (see Figure 4.1):*

$$\bigoplus_{m\in\mathcal{I}_{(n,s)}} p_s\left(U^m\otimes S_i\right)$$

2. *and a subcomplex with homology $\mathcal{T}^-$:*

$$\bigoplus_{m\in\mathcal{J}_{(n,s)}} \left\langle p_s\left(U^m\otimes S_i\right), p_s\left(U^m\otimes r_i\right)\right\rangle.$$

Where

$$\mathcal{I}_{(n,s)} = \mathcal{K}\cap\{m\in\mathbb{Z}|0 > max(\mathcal{F}\left(U^m\otimes r_i\right)-(0,s))\} \tag{4.1}$$

and

$$\mathcal{J}_{(n,s)} = \mathcal{K} \cap \{m \in \mathbb{Z} | 0 \leq max(\mathcal{F}(U^m \otimes r_i) - (0,s))\} \tag{4.2}$$

for

$$\mathcal{K} = \left\{ m \in \mathbb{Z} \middle| \begin{array}{ll} m > & \frac{i^2-i}{2} - \frac{n-|i|-(s-i)+1}{2} \quad \text{if } n-|i|-(s-i) \text{ is odd} \\ m > & \frac{i^2-i}{2} - \frac{n-|i|-(s-i)}{2} \quad \text{if } n-|i|-(s-i) \text{ is even} \end{array} \right\} \tag{4.3}$$

The max is between the two coordinates of the filtration level for a fixed i and s. See Figure 4.1 for an example of $\bigoplus_{m \in \mathcal{I}_{(n,s)}} p_s(U^m \otimes S_i)$.

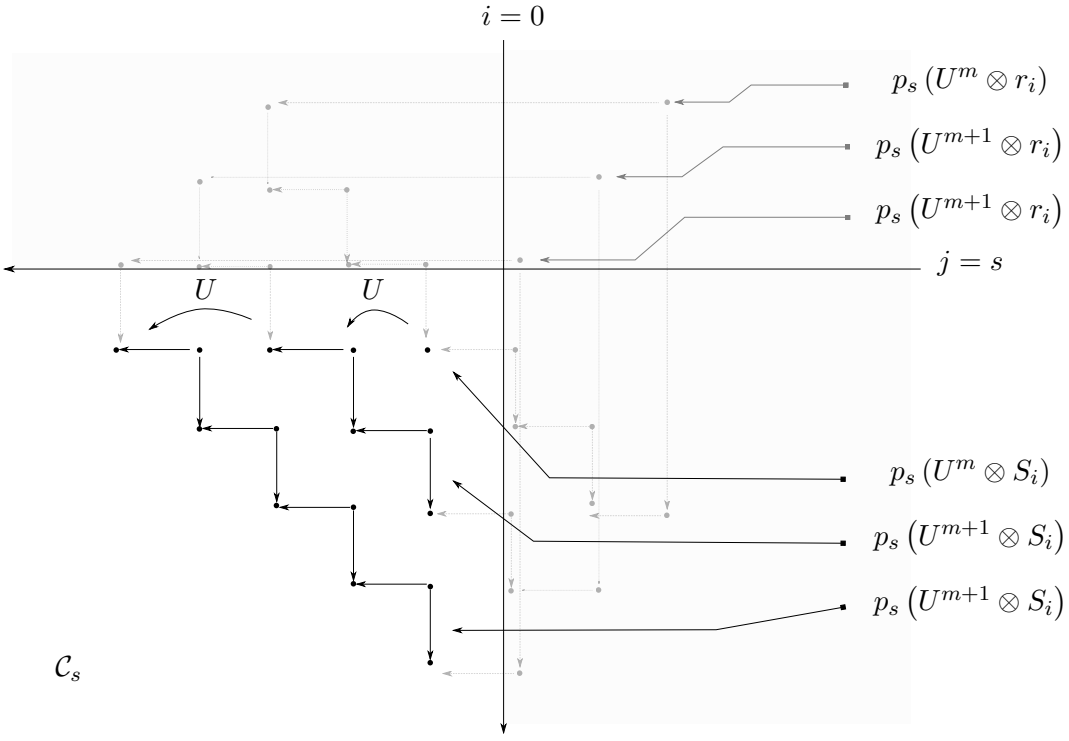

Figure 4.1: An example of $\bigoplus_{m \in \mathcal{I}_{(n,s)}} p_s(U^m \otimes S_i)$ with $|\mathcal{I}_{(n,s)}| = 3$. The unshaded area is $\mathcal{C}_s$.

Proof. Recall $\mathcal{C}_s$ is defined as the subcomplex of CFK^∞ generated by ele-

ments with filtration level less than $(0, s)$ and that the U-action lowers the filtration level by $(1, 1)$,

$$\mathcal{F}(U^m \otimes a) = \mathcal{F}(a) - (m, m)$$

Proposition 3.3.13 gives the filtration level of $p_s(U^m \otimes r_i) \neq 0$ explicitly:

$$\mathcal{F}(U^m \otimes r_i) = (\frac{i^2 - i}{2}, \frac{i^2 + i}{2}) - (m, m).$$

This gives us a simple way to predict the vanishing of $p_s(U^m \otimes r_i)$:

$$\begin{gathered} p_s(U^m \otimes r_i) \neq 0 \\ \Leftrightarrow \\ 0 > \max(\mathcal{F}(U^m \otimes r_i) - (0, s)) \end{gathered} \tag{4.4}$$

(Recall, the max is between the two coordinates of the filtration level for a fixed i and s.)

When $s = i$, both the corner $(0, s)$ of $\mathcal{C}_s$ and the $p_s(U^m \otimes r_i)$ lie on $y = x + s$ and multiplication by U translates along the line (See figure 4.2). The formula simplifies to:

$$\begin{gathered} p_s(U^m \otimes r_i) \neq 0 \\ \Leftrightarrow \\ m > \tfrac{i^2 - i}{2} \end{gathered} \tag{4.5}$$

Theorem 3.3.14 gives the relative filtration levels between $U^m \otimes S_i$ and the $U^m \otimes r_i$. We represent their relative filtration levels pictorially by an approximating right angled isosceles triangle (figure 4.3). $U^m \otimes r_i$ lies at the

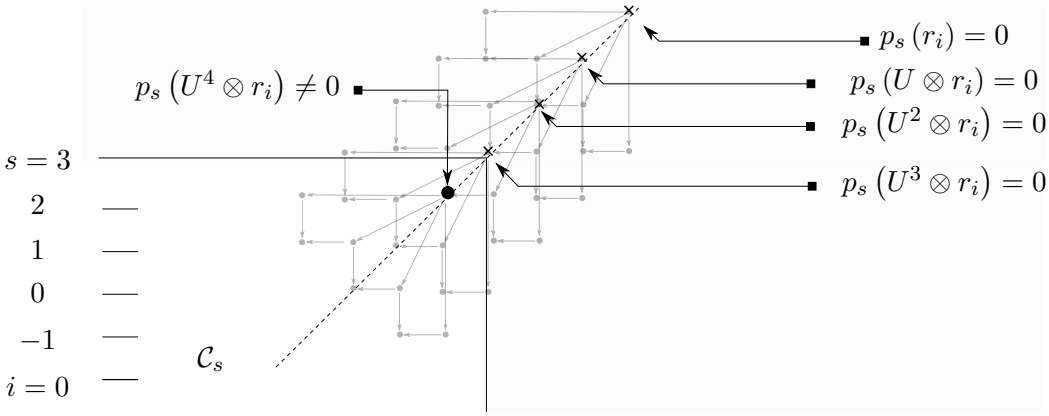

Figure 4.2: The unshaded area is the subcomplex $\mathcal{C}_s$. The exponent m of $U^m \otimes r_3$ must be strictly greater than $3 = \frac{3^2-3}{2}$ for $p_3(U^m \otimes r_3) \neq 0$.

corner of the right angle, the legs have length $n - i$, and the rail $U^m \otimes S_i$ lies approximately on the hypotenuse.

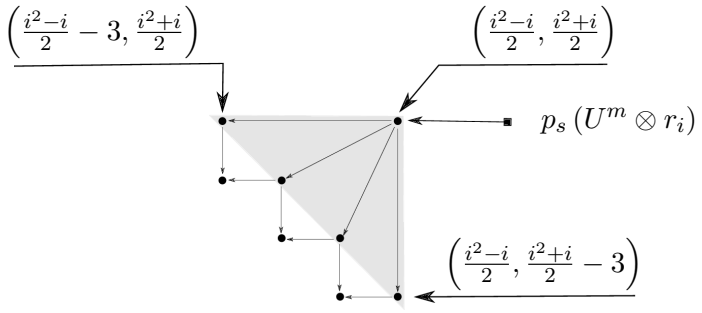

Figure 4.3: A visual representation of the relative filtration levels between $U^m \otimes r_i$ and $U^m \otimes S_i$. The approximating isosceles right triangle is shaded.

Using the relative filtration levels between $U^m \otimes S_i$ and $U^m \otimes r_i$ we derive a non-vanishing condition for $p_s(U^m \otimes S_i)$ as well.

The idea is to is to adjust the vanishing condition for $p_s(U^m \otimes r_i)$ by a quantity proportional to the height of the approximating triangle.

First we will look at the case when the index of the $U^m \otimes S_i$ and $U^m \otimes r_i$ are equal to the index of $\mathcal{C}_s$, namely when $i = s$. The calculation then generalizes easily by induction to the case $i \neq s$.

There are two cases based on the parity of $n - |i|$.

1. If $n-|i|$ is odd, the center of $U^m \otimes S_i$ is a 'pushed in corner' (figure 4.4). $p_s\left(U^m \otimes S_i\right) \neq 0$ if and only if

$$m > \frac{i^2 - i}{2} - \frac{n - |i| + 1}{2} \tag{4.6}$$

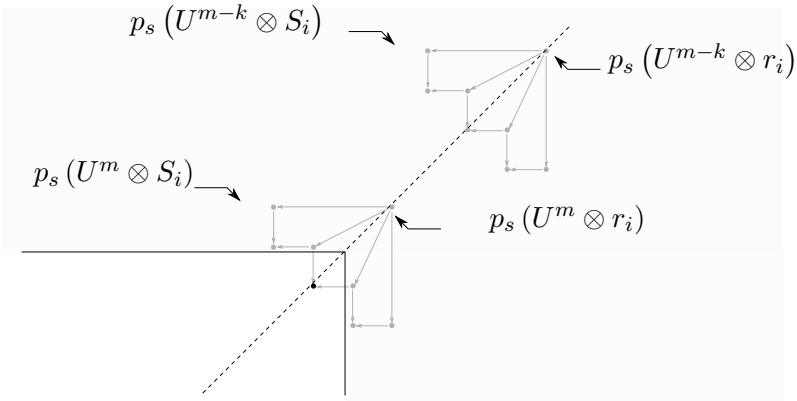

Figure 4.4: A pushed in middle corner. This happens when the length ($n-|i| = 3$ here) of the triangle is an even integer

2. If $n - i$ is even, the center of $U^m \otimes S_i$ is a 'pushed out corner' (figure 4.5). $p_s\left(U^m \otimes S_i\right) \neq 0$ if and only if

$$m > \frac{i^2 - i}{2} - \frac{n - |i|}{2} \tag{4.7}$$

Now for $s \neq i$. We can see this by keeping i constant and shifting s (figure 4.6). It's easy to see that shifting s up or down corresponds to increasing

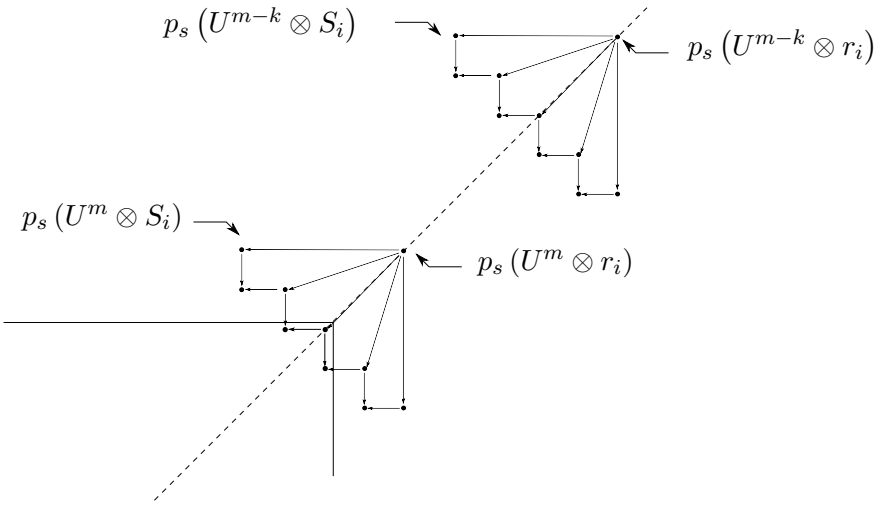

Figure 4.5: A pushed out middle corner. This happens when the length of the triangle is an odd integer

or decreasing the length of the projected rail by one. Likewise, changing the exponent m increases or decreases the length of the projected rail. As the vanishing conditions for the projected rail are given in terms of the exponent, We can get the general case of $s \neq i$ by subtracting $s - i$ from the vanishing conditions for $s = i$. The general equations are then:

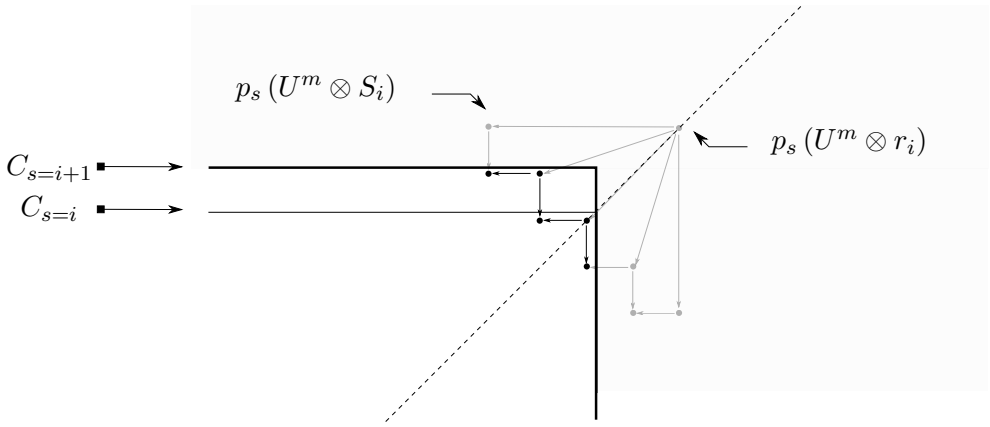

Figure 4.6: An example of two projections of holding the index i of $U^m \otimes S_i$ and $U^m \otimes r_i$ constant and shifting the index s of $p_{s=i}$ to $p_{s=i+1}$.

1.

$$m > \frac{i^2 - i}{2} - \frac{n - |i| - (s - i) + 1}{2} \text{ if } n - |i| - (s - i) \text{ is odd.} \tag{4.8}$$

2.

$$m > \frac{i^2 - i}{2} - \frac{n - |i| - (s - i)}{2} \text{ if } n - |i| - (s - i) \text{ is even.} \tag{4.9}$$

This verifies half of the corollary, namely that the subcomplex $\mathcal{C}_s$ consists of only those $p_s\left(U^m \otimes S_i\right)$ with exponents $m \in \mathcal{K}$

Now for the second part of the corollary. We show that if

$$p_s\left(U^m \otimes r_i\right) \neq 0$$

then

1. $p_s\left(U^m \otimes S_i\right) \neq 0$
2. $p_s\left(U^m \otimes r_j\right) \neq 0$ for $|k| < |i|$

Figure 4.7 is a pictoral illustration of the complex.

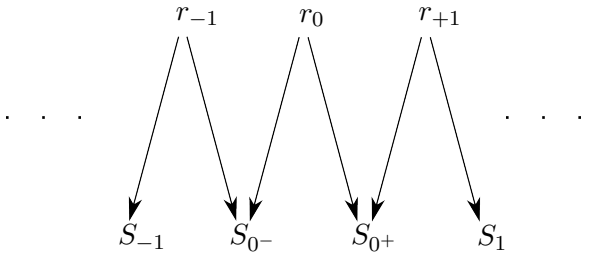

Figure 4.7: A pictoral representation of the subcomplex of C_i containing all of the non-vanishing $p\left(r_i\right)$.

Notice that if $(\frac{j^2-j}{2}, \frac{j^2-j}{2}) \in \mathcal{C}_s$ then $(\frac{j^2-j}{2}, \frac{j^2-j}{2}) \in \mathcal{C}_s$ for $|j| < |i|$ as

well. Since these are the filtration levels of the $p_s(U^m \otimes r_i)$, we have that if $\mathcal{F}(p_s(U^m \otimes r_i)) \in \mathcal{C}_s$, then

$$p_s(U^m \otimes r_j) \in \mathcal{C}_s \text{ for } |j| < |i|. \tag{4.10}$$

Since, every element in $p_s(S_i)$ has filtration level less than or equal to the filtration levels of (r_i), $\mathcal{C}_s$ also contains:

$$p_s\left(U^\ell \otimes S_j\right) \quad j \in \{-(|i|-1), ..., |i|\} \tag{4.11}$$

Putting the $p_s\left(U^\ell \otimes S_j\right)$ and $p_s\left(U^\ell \otimes j_j\right)$ together the resulting subcomplex looks as shown in figure 4.7.

The homology is computed analogously to our computation of the homology of CFK^∞ above. e.g. $\partial p_s\left(U^\ell \otimes r_j\right)$ equates the cycles from $p_j\left(U^\ell \otimes S_j\right)$, $p_j\left(U^\ell \otimes S_{j+1}\right)$:

$$\left[\sum_{c \in p_s(S_i)} U^\ell \otimes c\right] = \left[\sum_{c \in p_s(S_j)} U^\ell \otimes c\right]$$

□

[OS08] introduce two tricks to simplify the computation of $H_*(\mathbb{X}^+(1))$, 'truncation' (see lemma 2.0.16) and a condition under which we may identify a mapping cone with the kernel of its chain map.

The chain map $D^+_{1:n}$ is the sum of v_s and h_s. We analyze the maps these induce on homology, $(v_s)_*$, $(h_s)_*$. We start with a lemma on the structure of $B^+_s \cong CF^+$, whose homology is the range of $(v_s)_*$, $(h_s)_*$.

Lemma 4.0.19 *Let $\pi : CFK^\infty \longrightarrow CFK^+$ be the quotient map. Then*

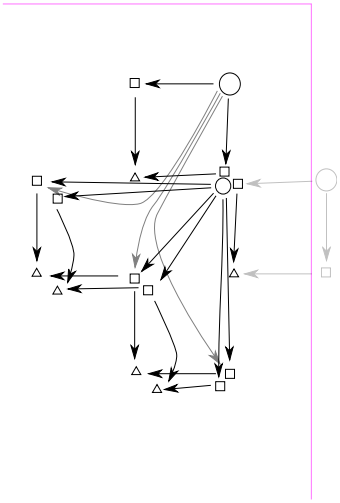

Figure 4.8: A projection of $U^m \otimes \mathcal{R}$ to $\mathcal{C}_s$ for a single m. The subcomplex generated by $p_s(S_i)$ and associated $p(r_i) \neq 0$ occupies most of the picture (figure 4.7 is a pictoral representation of it). There is a single rail on the right with zero homology (the right side of figure 3.16).

CFK^+ is quasi-isomorphic to the subcomplex:

$$\left\langle \cup_{m\geq 0} \left[\sum_{c\in\pi(U^m\otimes S_0)} c \right] \right\rangle$$

Proof. Since we are dealing with a knot in S^3, $H_*(CFK^+) = \mathcal{T}_0^+$ and π_* is a surjection.

Surjectivity of π_* lets us represent the cycles of CFK^+ by a quotient of the cycles of CFK^∞:

$$\pi(U^m \otimes S_0).$$

The restriction of $m \geq 0$ for the exponent follows from the filtration on CFK^∞. □

Proposition 4.0.20 *The induced maps on homology:*

$$(v_s)_* : H_*(A_s^+) \longrightarrow H_*(B_s^+)$$

$$(h_s)_* : H_*(A_s^+) \longrightarrow H_*(B_s^+)$$

are surjective and on $U^k \cdot H_*(A_s^+) \cong \mathcal{T}^+$ *for* $k >> 0$*, the maps can be identified with multiplication by* U^s *or the unit* 1 *(as* $H_*(B_s^+) \cong \mathcal{T}^+$ *as well):*

$$(h_s)_*, (v_{-s})_* = \begin{cases} 1 & s \leq 0 \\ U^s & s > 0 \end{cases}$$

Proof. For surjectivity: Let $p_s : CFK^\infty \longrightarrow A_s^+$ be the quotient map. Then, the quotient map $\pi : CFK^\infty \longrightarrow B_s^+ \cong CF^+$ factors, $\pi = v_s \circ p$. Thus:

$$\pi_* = (v_s \circ p)_* = (v_s)_* \circ (p)_*$$

Since π_* is a surjection, so is $(v_s)_*$. where v_s is the map between A_s^+ and B_s^+, and thus the induced map $(v_s)_*$ is surjective. Surjectivity of $(h_s)_*$ follows similarly (since you can think of it like $(v_s)_*$ by switching the the x and y axis and then shifting laterally).

Under (v_s), $[p_s(S_0)] \mapsto [\pi(S_0)]$. Corollary 4.0.19 tells us $[\pi(S_0)]$ is the homology class with the lowest degree in $H_*(B_s^+)$. Thus $(v_s)_*$ is injective on $U^k \cdot H_*(A_s^+) \cong \mathcal{T}^+, k >> 0$ for for $s > 0$.

More precisely, $(v_s)_*$, $(h_s)_*$ is given by U^j on $U^k \cdot H_*(A_s^+) \cong \mathcal{T}^+, k >> 0$, where $j \geq 0$ is the largest exponent such that $U^j \cdot [p_s(S_0)] \neq 0$

□

Proposition 4.0.21 *$H_*(\mathbb{X}^+(1)) \cong H_*(\mathbb{X}^+(1;n))) \cong ker\left(D^+_{1:n}\right)_*$ where n is the index of the cork boundary $-\partial W_n$.*

Proof. First we show that we can take $b = n$ where b is from lemma 2.0.16 and n is the index of our cork $-\partial W_n$.

This will follow if CFK^∞ lies between the lines $y = x + n$ and $y = x - n$, as this would imply $(v_s)_*$ is an isomorphism, for $s > n$ and also $(h_s)_*$ when $s < n$.

Let the rail S_i lie below the line $y = x+C_i$, and S_j below $y = x+C_j$ (where C_i an C_j are taken to be the smallest integer possible). Then by looking at the filtration levels of theorem 3.3.14, we get $C_i - C_j = i - j$. In particular, S_i lies below $y = x + C_j$ if $j \geq i$. Thus all the rails lie below $y = x + C_{n-1}$. Theorem 3.3.14 lets us calculate $C_{n-1} = n$. To finish off, note that the $r_i \in \mathcal{R}$ also lie below this line as $\mathcal{F}(r_i) = \left(\frac{i^2-i}{2}, \frac{i^2+i}{2}\right)$ and $-(n-1) \leq i \leq n-1$.

By the symmetry of CFK^∞ around $y = x$, nothing lies below $y = x - n$. This finishes the argument for truncation.

Now we identify $H_*(\mathbb{X}^+(1;n))$ with the kernel of $D^+_{1;n} : H_*(\mathbb{A}^+(n)) \longrightarrow H_*(\mathbb{B}^+(n))$. Since the homology of the mapping cone of $f : X \longrightarrow Y$ is isomorphic to the kernel of $f_* : H_*(X) \longrightarrow H_*(Y)$ if f_* is surjective, the claim will follow if the chain map $\left(D^+_{1:n}\right)_*$ of $\mathbb{X}^+(1;n)$ is surjective.

Recall $D^+_{1:n}$ is the restriction of $\bigoplus_s v_s \oplus h_s$ to the truncated mapping cone $\mathbb{X}^+(1;n)$. See figure 4.9.

The preceding proposition, 4.0.20, showed the induced maps on homology:

$$(v_s)_* : H_*(A^+_s) \longrightarrow H_*(B^+_s)$$

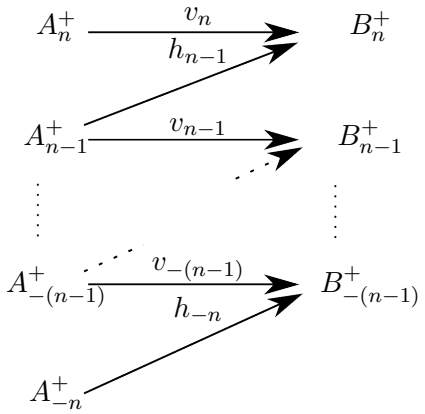

Figure 4.9: $D_{1:n}^+$. Surjectivity of each of the v_s, h_s implies surjectivity of $D_{1:n}^+$ walking the surjectivity of h_{-n} up to the top by adding the $v_s \oplus h_s$ one at a time.

$$(h_s)_* : H_*(A_s^+) \longrightarrow H_*(B_s^+)$$

are surjective.

Using linear combinations of the $(v_s)_*$ and $(h_s)_*$ we can bootstrap this into surjectivity of $\left(D_{1:n}^+\right)_*$.

Since

$$\{0 \oplus ...0 \oplus H_*\left(B_i^+\right) \oplus 0... \oplus 0\}_{-(n-1)<i<n}$$

span $\bigoplus_{\{-n<s<n\}} H_*\left(B_s^+\right)$, it is enough to show each of these sub-spaces is in the image of $\left(D_{1:n}^+\right)_*$.

The restriction of $\left(D_{1:n}^+\right)_*$ to the submodule

$$0 \oplus ... \oplus 0 \oplus H_*\left(A_{-n}^+\right)$$

is the map:

$$\begin{aligned} &0 \oplus ... \oplus 0 \oplus (h_{-n})_* \oplus (v_{-n})_* \\ =&0 \oplus ... \oplus 0 \oplus (h_{-n})_* \end{aligned}$$

This follows as $H_*\left(B^+_{-(n-1)}\right)$ is the lowest possible index $-(n-1)$ and thus $(v_{-n})_* = 0$ (as its intended target, $H_*\left(B^+_{-n}\right)$ is truncated. See bottom of figure 4.9).

In the case of when $s > -n$, the restriction of $\left(D^+_{1:n}\right)_*$ to the submodule

$$0 \oplus ... \oplus 0 \oplus H_*\left(B^+_{s+1}\right) \oplus H_*\left(B^+_s\right) \oplus ... \oplus 0$$

has image:

$$0 \oplus ... \oplus 0 \oplus H_*\left(A^+_{-n}\right)$$

as $(v_n)_* \neq 0$.

However if the single summand

$$0 \oplus ... \oplus 0 \oplus H_*\left(B^+_s\right) \oplus ... \oplus 0$$

is in the image, the linearity of $\left(D^+_{1:n}\right)_*$ implies

$$0 \oplus ... \oplus 0 \oplus H_*\left(B^+_{s+1}\right) \oplus ... \oplus 0$$

is also in the image.

Since there are a finite number of

$$0 \oplus ... \oplus 0 \oplus H_* \left(B_s^+ \right) \oplus ... \oplus 0$$

we can induct off of

$$0 \oplus ... \oplus 0 \oplus H_* \left(A_{-n}^+ \right)$$

and conclude surjectivity. □

Theorem 4.0.22

$$\begin{aligned} H_* \left(\mathbb{X}(n) \right) =& \mathcal{T}_0^+ \oplus \bigoplus_{-n<s<n} \left(\frac{\mathbb{F}[U]}{U^{m(s,0)}\mathbb{F}[U]} \right)^2_{((s^2-s)-(i^2-i)-min(0,2(i-s)))} \\ & \oplus \left(\bigoplus_{\{m(s,i)>0, i\neq 0\}} \frac{\mathbb{F}[U]}{U^{m(s,i)}\mathbb{F}[U]} \right)_{((s^2-s)-(i^2-i)-min(0,2(i-s)))} \end{aligned}$$

Where

$$m(s,i) = \begin{cases} min\left(0,(i-s)\right) - \frac{n-|i|-(s-i)+1}{2} & \text{if } n-|i|-(s-i) \text{ is odd} \\ min\left(0,(i-s)\right) - \frac{n-|i|-(s-i)}{2} & \text{if } n-|i|-(s-i) \text{ is even} \end{cases} \tag{4.12}$$

Note: $|i|, |s|$ *must be* $< n$ *by theorem 3.3.14.*

Proof. By theorem 2.0.12, $H_* \left(-\partial W_n \right)$ is given by the homology of the mapping cone of $D_1^+ : \mathbb{A}^+ \longrightarrow \mathbb{B}^+$. Proposition 4.0.21 tells us this is given by

$\ker\left(D^+_{1:n}\right)_*$. Since $H^{\mathrm{Red}}_*\left(A^+_s\right) \leq \ker(v_s)_* \cap \ker(h_s)_*$ we may write this as:

$$\ker\left(D^+_{1:n}\right)_* \cong \bigoplus_s H^{\mathrm{Red}}_*\left(A^+_s\right) \oplus \mathcal{B}$$

Where $\mathcal{B}$ is the kernel of

$$\left(D^+_{1:n}\right)_* : \bigoplus_{-n\leq s\leq n} U^k \cdot H_*\left(A^+_s\right) \longrightarrow \bigoplus_{-(n-1)\leq s\leq n} H_*\left(B^+_s\right)$$

with $k >> 0$.

Proposition 4.0.20 shows that for each s, either $(v_s)^{\mathrm{Red}}_*$ or $(h_s)^{\mathrm{Red}}_*$ is an isomorphism. This lets us further truncate our mapping cone down to a single $\mathcal{T}^+_0$ in the domain and a map into 0.

Thus, $H_*\left(\mathbb{X}^+\right) \cong \mathcal{T}^+_0 \bigoplus_s H^{\mathrm{Red}}_*\left(A^+_s\right)$.

Proposition 4.0.17 gives us an isomorphism between $H^{\mathrm{Red}}_*\left(A^+_s\right)$ and $H^{\mathrm{Red}}_*\left(\mathcal{C}_s\right)$. Corollary 4.0.18, showed $H^{\mathrm{Red}}_*\left(\mathcal{C}_s\right)$ is given by the homology of a direct sum of rails:

$$H^{\mathrm{Red}}_*\left(\mathcal{C}_s\right) \cong H_s\left(\bigoplus_i \bigoplus_{m\in\mathcal{I}_{(n,s)}} p_s\left(U^m \otimes S_i\right)\right)$$

For a fixed i, the subcomplexes consisting only of rails $p_s\left(U^m \otimes C_i\right)$ will form a submodule in $H^{\mathrm{Red}}_*\left(\mathcal{C}_s\right)$, $\frac{\mathbb{F}[U]}{U^m\cdot\mathbb{F}[U]}$.

The exponent m is calculated by counting the number of rails that have non-trivial homology. A rail is acyclic if and only if it has an even number of generators: $2|\#\{p_s\left(U^m \otimes S_i\right)\}$. (See figure 4.10). This happens if and only if:

$$0 < \min\left[\mathcal{F}(U^m \otimes r_i) - (0,s)\right] \tag{4.13}$$

otherwise its homology is:

$$H_* \left(U^m \otimes S) \right) = \mathbb{F}$$

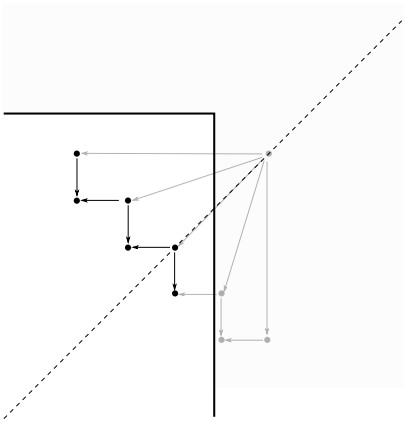

Figure 4.10: An example of an acyclic rail $p_s \left(U^m \otimes S_i \right)$ with $m < \frac{i^2-i}{2} + \min\left(0, i-s\right)$.

Now equation 4.13 becomes 4.14

$$\begin{aligned} 0 &< \min\left[\mathcal{F}(U^m \otimes r_i) - (0,s)\right] \\ &< \min\left(\frac{i^2-i}{2} - m, \frac{i^2+i}{2} - m - s\right) \\ &\Leftrightarrow \\ m &< \min\left(\frac{i^2-i}{2}, \frac{i^2+i}{2} - s\right) \end{aligned}$$

$$m < \frac{i^2-i}{2} + \min\left(0, i-s\right) \tag{4.14}$$

Thus the homology isomorphic to the underlying chain complex modulo the rails $p_s\left(U^m \otimes S_i\right)$ with $m < \frac{i^2-i}{2} + \min\left(0, i-s\right)$.

The absolute homological grading is given by adjusting $H_*^{\mathrm{Red}}\left(\mathcal{C}_s\right)$ by s^2-s. (Theorem 2.0.12 tells us to shift A_s^+ by s^2-s+1 and the boundary map in the L.E.S. relating $H_*^{\mathrm{Red}}\left(A_s^+\right)$ and $H_*^{\mathrm{Red}}\left(\mathcal{C}_s\right)$ drops this to a shift by s^2-s.) The powers of U^m correspond to changing this grading by two so we must multiply by two before shifting by s^2-s.

For a given s, i, this gives:

$$\frac{\mathbb{F}[U]}{U^{m(s,i)} \otimes \mathbb{F}[U]}_{((s^2-s)-(i^2-i)-\min(0,2(i-s)))}$$

With

$$m(s,i) = \begin{cases} \min\left(0,(i-s)\right) - \frac{n-|i|-(s-i)+1}{2} & \text{if } n-|i|-(s-i) \text{ is odd} \\ \min\left(0,(i-s)\right) - \frac{n-|i|-(s-i)}{2} & \text{if } n-|i|-(s-i) \text{ is even} \end{cases} \tag{4.15}$$

Putting all these subcomplexes together and remembering to double count when $i=0$, gives the result. □

Example 4.0.23 *$HF^+\left(-\partial W_1\right)$. Plugging into the formula,*

$$\begin{aligned} H_*\left(\mathbb{X}(n)\right) &= \left(\frac{\mathbb{F}[U]}{U^{m(0,0)=\left\lfloor \frac{1-|0|+1-|0-0|}{2} \right\rfloor}\mathbb{F}[U]}\right)_0^2 \oplus \mathcal{T}_0^+ \\ &= \left(\frac{\mathbb{F}[U]}{U \cdot \mathbb{F}[U]}\right)_0^2 \oplus \mathcal{T}_0^+ \end{aligned}$$

Chapter 5

Further Directions

5.1 Four-Manifold Invariant

The calculation of $HF^+(-\partial W_n)$ is the first step in computing the four-manifold invariant:

$$F^+_{W_n(K)} : HF^+(-\partial W_n) \longrightarrow HF^+\left(S^3\right).$$

[OS08] gives the cobordism map

$$F^+_{W_n(K)} : HF^+\left(S^3\right) \longrightarrow HF^+(-\partial W_n)$$

as the map induced on homology by the inclusion:

$$\iota_* : H_*(B_0) \longrightarrow H_*\left(\mathbb{X}^+(n)\right).$$

One would hope for a similar result for the cobordism map

$$F^+_{W_n(K)} : HF^+\left(-\partial W_n\right) \longrightarrow HF^+\left(S^3\right).$$

Namely, for it to be given as the map induced on homology by the projection:

$$\pi_* : H_*\left(\mathbb{X}^+(n)\right) \longrightarrow H_*\left(B_0\right).$$

In principal this should be more time consuming than hard. In conversation, Peter Ozsváth suggested it could be done by redoing [OS08] using the subcomplex $\frac{CFK^\infty}{CFK^\infty\{i<0 \text{ or } j<s\}}$ instead of $A^+_s = \frac{CFK^\infty}{CFK^\infty\{i<0 \text{ and } j<s\}}$.

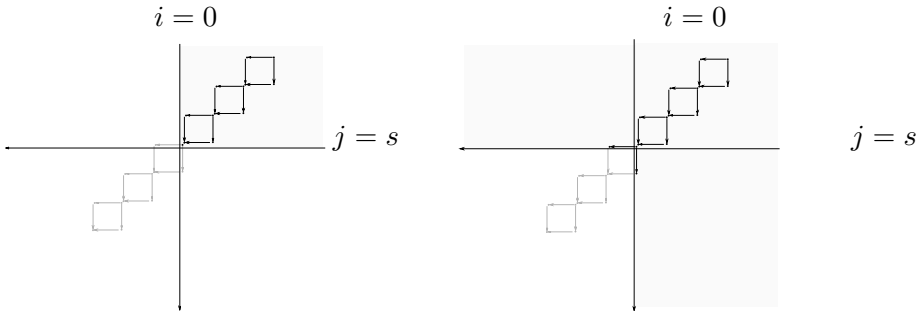

Figure 5.1: $\frac{CFK^\infty}{CFK^\infty\{i<0 \text{ or } j<s\}}$ on the left instead of $A^+_s = \frac{CFK^\infty}{CFK^\infty\{i<0 \text{ and } j<s\}}$ on the right.

5.2 Cork Twist Cobordism

The interest in corks arises from the difference that arise between attaching it via the identity map or via the twist τ.

A natural way to approach this it to compute map induced by the cobordism between a cork and its twist by τ_*.

This approach has already had some significant successes. In [AD05] they

looked at the Mazur cork $-\partial W_n$ and showed that τ_*, acts non-trivially on its Heegaard Floer homology.

In [AK11] τ_* was shown to act non-trivially on the contact invariant.

The information carried by the cork twist τ has thus not been lost by passing to Floer homology. Further, because τ_*'s action on the contact invariant is non-trivial, there is reason to hope the Heegaard Floer invariant may be picking up an interesting aspect of the corks.

With the Floer homology of the corks computed, one could hope that the cobordism maps could be computed directly from the diagram. The hope being that the differential on the Heegaard diagram could be computed explicitly by reasoning backwards from what we know the Floer homology must be.

5.3 New Exotic Manifolds

Even with a full understanding of the Heegaard invariants of corks construction or detection of new exotic manifolds would pose difficulties. To compute the Heegaard Floer invariant of a four-manifold X, you need information not only about the cork W, but also $X - W$.

To sidestep this, one idea is to modify manifolds, that work well with some of the Mazur corks, to produce manifolds which work well with other Mazur corks.

Let B denote the cobordism representing the boundary map in the surgery exact sequence shown in Figure 5.2. (There is an analogous sequence for Positron corks.) By computing the Heegaard Floer invariant of B we could ask: if W is a cork in a smooth four-manifold $W = M \cup W$, is W' was also a

cork in $M' = M \cup B \cup W'$?

One would hope to find a large number of new exotic manifolds by iterating this process of 'stacking' corks.

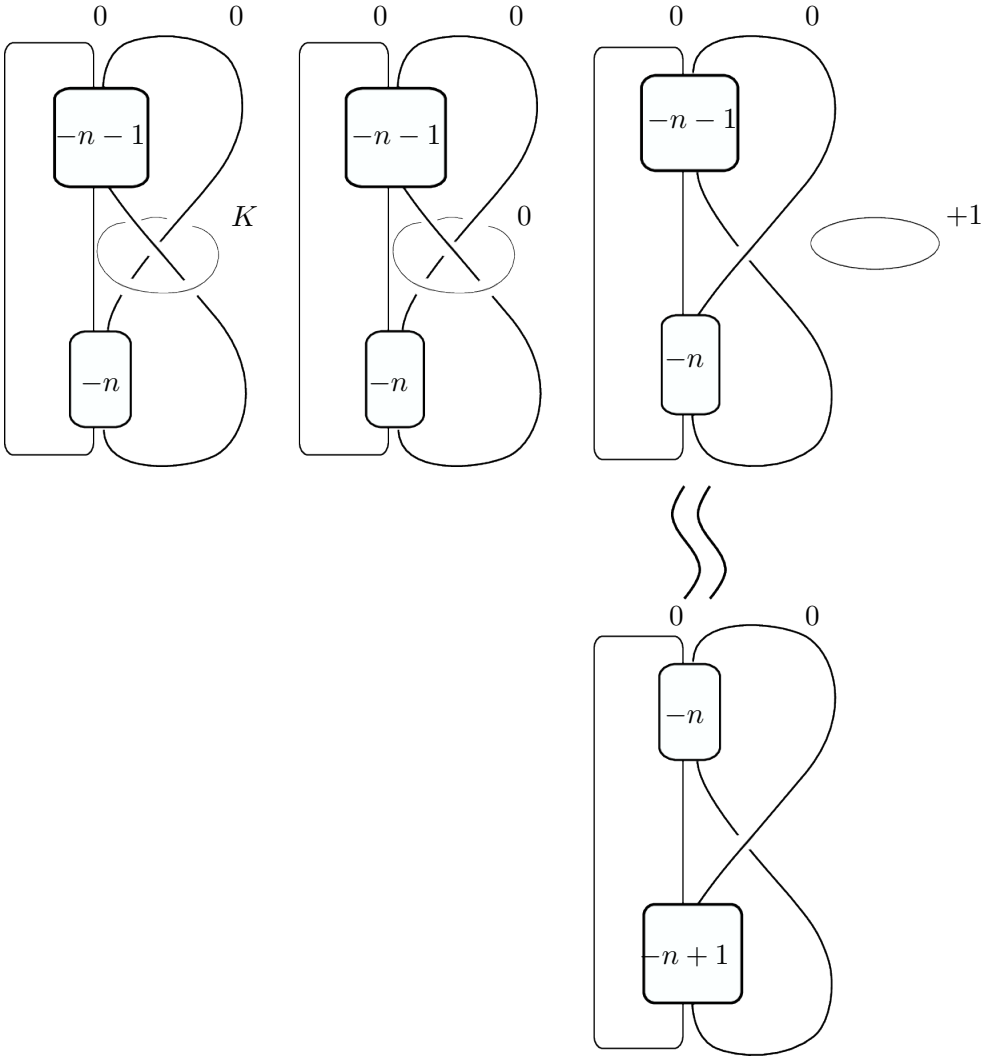

Figure 5.2: +1 surgery along the knot K gives a surgery triangle containing $-\partial W_n$ and $-\partial W_{n-1}$.

5.4 More corks

This approach to the computation of the invariant is extendible to other corks as well. Even if a closed formula is not obtainable, one should be able obtain an algorithm. As an example, the computation of the first cork of the Positron family is sketched.

Following the procedure for reducing the surgery to a knot, we get Figure 5.4 from the two bridge link in Figure 5.3. We build the complex by inspection then compute $H_*(A_s^+)$.

From Figure 5.7 we get:

$$H_*(A_{\pm 1}^+) = \mathbb{F}_{(2)}$$

and

$$H_*(A_{\pm 0}^+) = \mathbb{F}_{(0)} \oplus \mathbb{F}_{(0)}$$

So

$$HF^+\left(-\partial\overline{W_1}\right) = \mathcal{T}_0^+ \oplus \left(\mathbb{F}_{(0)} \oplus \mathbb{F}_{(0)}\right) \oplus \left(\mathbb{F}_{(2)} \oplus \mathbb{F}_{(2)}\right)$$

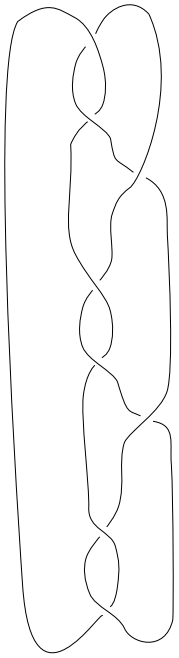

Figure 5.3: Kirby Diagram of $-\partial\overline{W_1}$

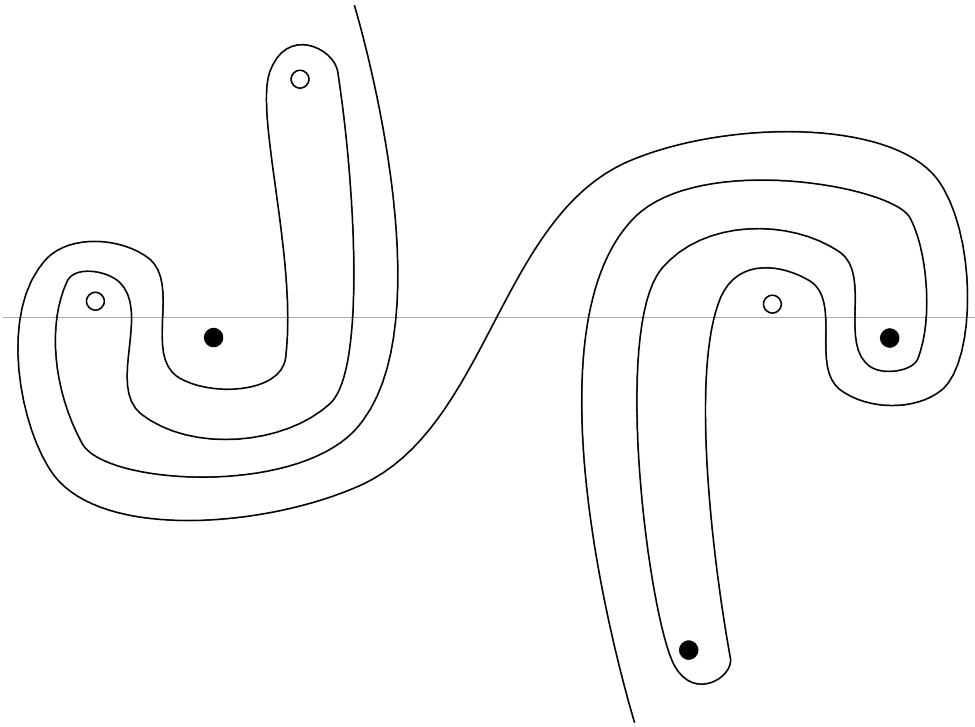

Figure 5.4: Heegaard Diagram for CFK^∞ of the knot associated to $-\partial\overline{W_1}$

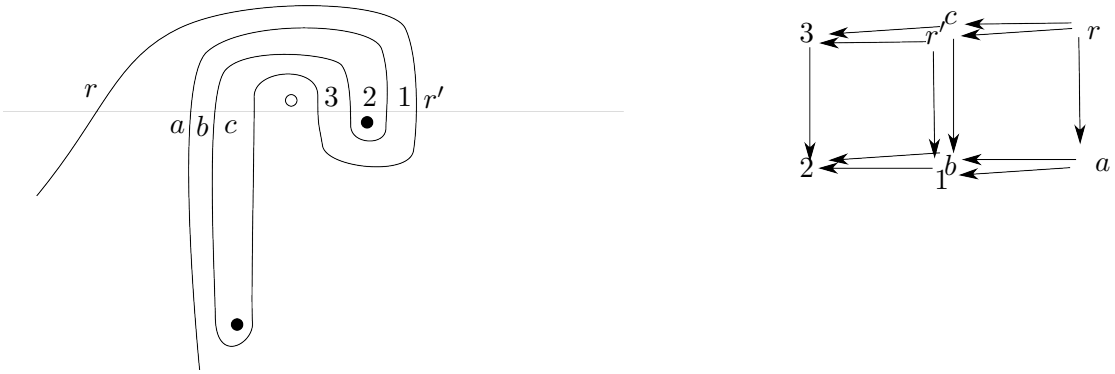

Figure 5.5: Detail of the Heegaard diagram with labeling corresponding to the chain complex below

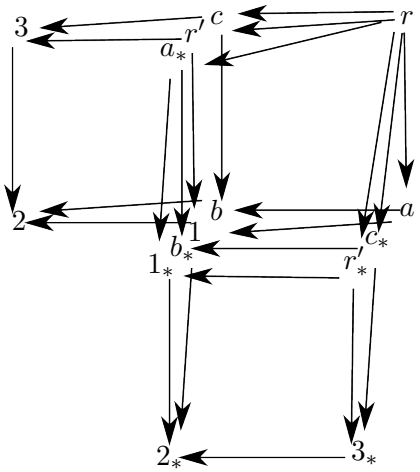

Figure 5.6: $\mathcal{R}$ where $CFK^\infty = \mathbb{F}[U, U^{-1}] \otimes \mathcal{R}$. The subscript $*$ denotes generators from the other half of the Heegaard diagram.

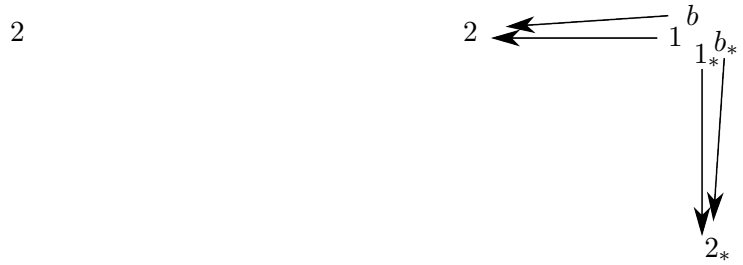

Figure 5.7: A_1^+ on the left (the number 2 signifies a single element with no differentials) and A_0 on the right.

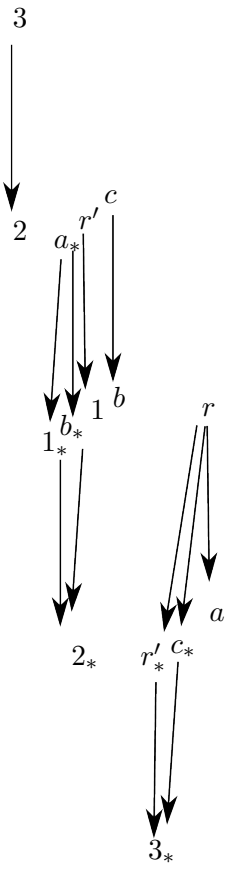

Figure 5.8: $\widehat{CF}$

Bibliography

[AD05] Selman Akbulut and Selahi Durusoy. An involution acting non-trivially on Heegaard-Floer homology. *Fields Institute Communications*, 47:1–9, 2005.

[AK11] Selman Akbulut and Cagri Karakurt. Action of the cork twist on Floer homology. *arXiv preprint arXiv:1104.2247*, 2011.

[AK12] Selman Akbulut and Cagri Karakurt. Heegaard Floer homology of some mazur type manifolds. *arXiv preprint arXiv:1204.3862*, 2012.

[Akb91] Selman Akbulut. A fake compact contractible 4-manifold. *J. Differential Geom*, 33(2):335–356, 1991.

[AY08] Selman Akbulut and Kouichi Yasui. Corks, plugs and exotic structures. *arXiv preprint arXiv:0806.3010*, 2008.

[Don83] SK Donaldson. Self-dual connections and the topology of smooth 4-manifolds. *Bulletin of the American Mathematical Society*, 8(1):81–83, 1983.

[Don85] S Donaldson. La topologie differentielle des surfaces complexes. *CR Acad. Sci. Paris*, 301(1):317–320, 1985.

[Don87] SK Donaldson. Irrationality and the h-cobordism conjecture. *J. Differential Geom*, 26(1):141–168, 1987.

[Fre82] Michael Hartley Freedman. The topology of four-dimensional manifolds. *J. Differential Geom*, 17(3):357–453, 1982.

[GS99] Robert E Gompf and András I Stipsicz. *4-manifolds and Kirby calculus*, volume 20. Amer Mathematical Society, 1999.

[Har13] Eric Harper. On instanton homology of corks W_n. *arXiv preprint arXiv:1304.5137*, 2013.

[JT12] András Juhász and Dylan P Thurston. Naturality and mapping class groups in Heegaard Floer homology. *arXiv preprint arXiv:1210.4996*, 2012.

[Kir97] Rob Kirby. Akbulut's corks and h-cobordisms of smooth simply connected 4-manifolds. *arXiv preprint math/9712231*, 1997.

[KLT10] Cagatay Kutluhan, Yi-Jen Lee, and Clifford Henry Taubes. HF= HM I: Heegaard Floer homology and Seiberg–Witten Floer homology. *arXiv preprint arXiv:1007.1979*, 2010.

[Lip06] Robert Lipshitz. A cylindrical reformulation of Heegaard Floer homology. *Geometry & Topology*, 10:955–1096, 2006.

[OS03] Peter Ozsváth and Zoltán Szabó. Absolutely graded Floer homologies and intersection forms for four-manifolds with boundary. *Advances in Mathematics*, 173(2):179–261, 2003.

[OS04a] Peter Ozsváth and Zoltán Szabó. Holomorphic disks and knot invariants. *Advances in Mathematics*, 186(1):58–116, 2004.

[OS04b] Peter Ozsváth and Zoltán Szabó. Holomorphic disks and knot invariants. *Advances in Mathematics*, 186(1):58–116, 2004.

[OS04c] Peter Ozsváth and Zoltán Szabó. Holomorphic disks and three-manifold invariants: properties and applications. *Annals of mathematics*, pages 1159–1245, 2004.

[OS04d] Peter Ozsváth and Zoltán Szabó. Holomorphic disks and topological invariants for closed three-manifolds. *Annals of Mathematics*, pages 1027–1158, 2004.

[OS06] Peter Ozsváth and Zoltán Szabó. Holomorphic triangles and invariants for smooth four-manifolds. *Advances in Mathematics*, 202(2):326–400, 2006.

[OS08] Peter Ozsváth and Zoltán Szabó. Knot Floer homology and integer surgeries. *Algebraic & Geometric Topology*, 8:101–153, 2008.

[Sma61] Stephen Smale. Generalized Poincaré's conjecture in dimensions greater than four. *The Annals of Mathematics*, 74(2):391–406, 1961.